Conversion of Carbon Dioxide to Methanol Using a C-H Activated Bis(imino)pyridine Molybdenum Hydroboration Catalyst

Supporting Information

*Raja Pal, Thomas L. Groy, Ryan J. Trovitch**

Department of Chemistry & Biochemistry, Arizona State University, Tempe, Arizona 85287

ryan.trovitch@asu.edu

Table S1. Crystallographic Data for **[(^{Ph_2PPr}PDI)MoI][I]** and **(κ^6-*P,N,N,N,C,P*-^{Ph_2PPr}PDI)MoH**.

	[(^{Ph_2PPr}PDI)MoI][I]	**(κ^6-*P,N,N,N,C,P*-^{Ph_2PPr}PDI)MoH**
chemical formula	$C_{39}H_{41}N_3I_2MoP_2$	$2(C_{39}H_{41}N_3MoP_2)$, C_7H_7
formula weight	963.43	1510.38
crystal dimensions	0.576 x 0.133 x 0.119	0.200 x 0.180 x 0.050
crystal system	orthorhombic	triclinic
space group	$P2_12_12_1$	$P\bar{1}$
a (Å)	10.270(5)	10.3197(12)
b (Å)	18.930(10)	13.0922(15)
c (Å)	19.310(10)	14.2479(17)
α (deg)	90	81.129(4)
β (deg)	90	82.476(3)
γ (deg)	90	76.341(3)
V (Å^3)	3754.(3)	1839.2(4)
Z	4	4
T (°C)	123.(2)	123.(2)
ρcalcd (g cm^{-3})	1.705	1.364
μ (mm^{-1})	2.111	0.478
reflections collected	29746	19605
data/restraints/parameters	6929/0/426	6213/13/425
R_1 [I > 2σ(I)]	0.0515	0.0776
wR_2 (all data)	0.1273	0.1734
Goodness-of-fit	1.028	1.069
Largest peak, hole (eÅ^{-3})	1.748, -0.608	2.628, -1.324

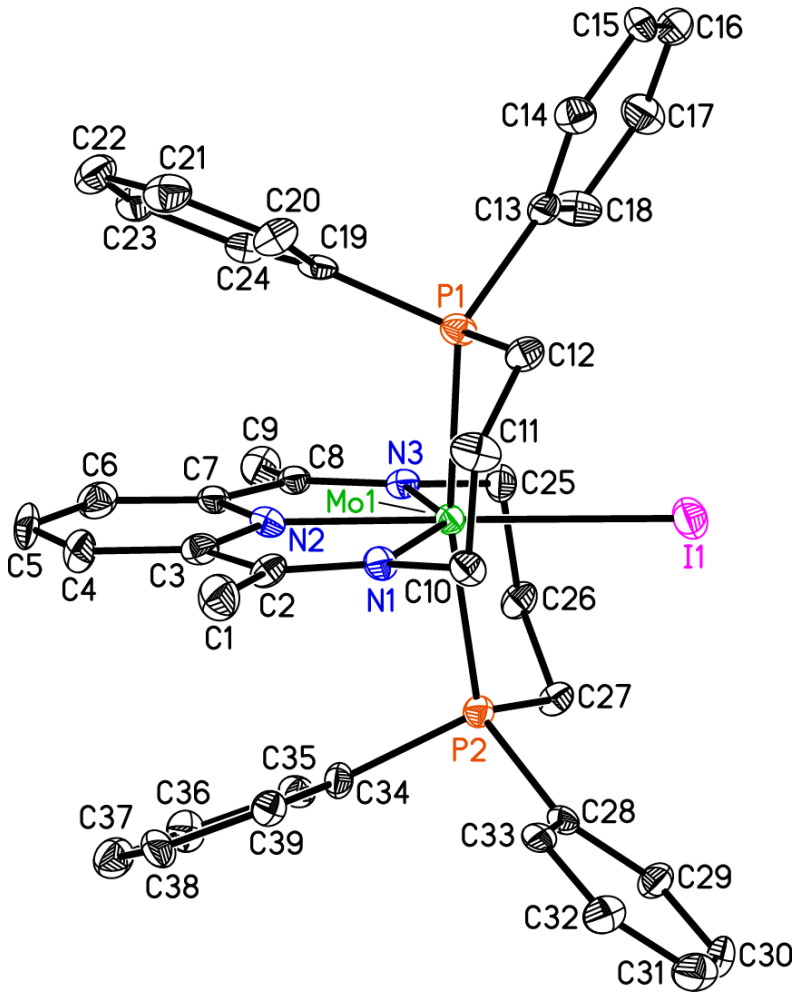

Figure S1. The molecular structure of **[(^{Ph_2PPr}PDI)MoI][I]** shown at 30% probability ellipsoids. Hydrogen atoms and I^- counterion are omitted for clarity.

Table S2. Metrical parameters for **[(^{Ph_2PPr}PDI)MoI][I]**.

Mo1-N1	2.036(11)	C1-C2	1.496(19)	C20-C21	1.35(2)
Mo1-N3	2.077(10)	C2-C3	1.442(17)	C21-C22	1.40(2)
Mo1-N2	2.112(10)	C3-C4	1.395(17)	C22-C23	1.38(2)
Mo1-P2	2.453(3)	C4-C5	1.363(18)	C23-C24	1.376(19)
Mo1-P1	2.472(3)	C5-C6	1.391(19)	C25-C26	1.525(17)
Mo1-I1	2.7810(17)	C6-C7	1.353(18)	C26-C27	1.567(16)
P1-C19	1.807(13)	C7-C8	1.401(18)	C28-C29	1.396(18)
P1-C13	1.834(13)	C8-C9	1.508(17)	C28-C33	1.408(18)
P1-C12	1.849(13)	C10-C11	1.521(17)	C29-C30	1.388(18)
P2-C28	1.835(12)	C11-C12	1.512(17)	C30-C31	1.34(2)
P2-C27	1.838(13)	C13-C18	1.380(18)	C31-C32	1.38(2)
P2-C34	1.839(12)	C13-C14	1.398(17)	C32-C33	1.382(17)
N1-C2	1.332(16)	C14-C15	1.390(17)	C34-C35	1.372(17)
N1-C10	1.498(15)	C15-C16	1.356(19)	C34-C39	1.400(17)
N2-C3	1.356(16)	C16-C17	1.346(19)	C35-C36	1.379(18)
N2-C7	1.368(15)	C17-C18	1.419(19)	C36-C37	1.37(2)
N3-C8	1.324(15)	C19-C20	1.410(18)	C37-C38	1.392(19)
N3-C25	1.474(16)	C19-C24	1.423(17)	C38-C39	1.380(17)

N1-Mo1-N3	141.6(4)	C3-N2-C7	117.7(11)	C16-C17-C18	121.2(15)
N1-Mo1-N2	70.8(4)	C3-N2-Mo1	121.3(8)	C13-C18-C17	118.3(12)
N3-Mo1-N2	70.9(4)	C7-N2-Mo1	120.9(8)	C20-C19-C24	118.1(12)
N1-Mo1-P2	100.8(3)	C8-N3-C25	122.2(10)	C20-C19-P1	124.9(10)
N3-Mo1-P2	80.3(3)	C8-N3-Mo1	123.3(8)	C24-C19-P1	117.1(10)
N2-Mo1-P2	95.4(3)	C25-N3-Mo1	113.8(8)	C21-C20-C19	120.2(13)
N1-Mo1-P1	80.2(3)	N1-C2-C3	110.3(11)	C20-C21-C22	121.7(14)
N3-Mo1-P1	105.7(3)	N1-C2-C1	125.3(11)	C23-C22-C21	118.9(14)
N2-Mo1-P1	95.0(3)	C3-C2-C1	124.4(12)	C24-C23-C22	120.7(13)
P2-Mo1-P1	169.30(12)	N2-C3-C4	121.4(11)	C23-C24-C19	120.4(13)
N1-Mo1-I1	110.8(3)	N2-C3-C2	111.5(11)	N3-C25-C26	112.6(10)
N3-Mo1-I1	107.6(3)	C4-C3-C2	127.1(11)	C25-C26-C27	113.6(10)
N2-Mo1-I1	178.2(3)	C5-C4-C3	120.4(12)	C26-C27-P2	118.4(8)
P2-Mo1-I1	83.48(9)	C4-C5-C6	117.5(12)	C29-C28-C33	118.2(11)
P1-Mo1-I1	86.22(9)	C7-C6-C5	121.2(12)	C29-C28-P2	123.0(9)
C19-P1-C13	104.0(5)	C6-C7-N2	121.8(12)	C33-C28-P2	118.6(9)
C19-P1-C12	105.9(6)	C6-C7-C8	126.6(12)	C30-C29-C28	120.4(13)
C13-P1-C12	102.3(5)	N2-C7-C8	111.6(11)	C31-C30-C29	119.9(14)
C19-P1-Mo1	113.6(4)	N3-C8-C7	113.3(10)	C30-C31-C32	122.0(13)
C13-P1-Mo1	122.3(4)	N3-C8-C9	123.0(12)	C31-C32-C33	119.2(14)
C12-P1-Mo1	107.1(4)	C7-C8-C9	123.5(11)	C32-C33-C28	120.3(13)
C28-P2-C27	103.5(6)	N1-C10-C11	110.8(10)	C35-C34-C39	120.5(12)
C28-P2-C34	105.7(5)	C12-C11-C10	115.3(11)	C35-C34-P2	122.0(10)
C27-P2-C34	107.1(6)	C11-C12-P1	116.7(9)	C39-C34-P2	117.1(9)
C28-P2-Mo1	119.1(4)	C18-C13-C14	119.5(12)	C34-C35-C36	119.4(13)
C27-P2-Mo1	110.3(4)	C18-C13-P1	119.3(9)	C37-C36-C35	122.2(13)
C34-P2-Mo1	110.4(4)	C14-C13-P1	121.2(10)	C36-C37-C38	117.5(14)
C2-N1-C10	119.7(10)	C15-C14-C13	120.2(13)	C39-C38-C37	122.0(14)
C2-N1-Mo1	126.0(8)	C16-C15-C14	120.0(12)	C38-C39-C34	118.4(12)
C10-N1-Mo1	113.6(8)	C17-C16-C15	120.8(13)		

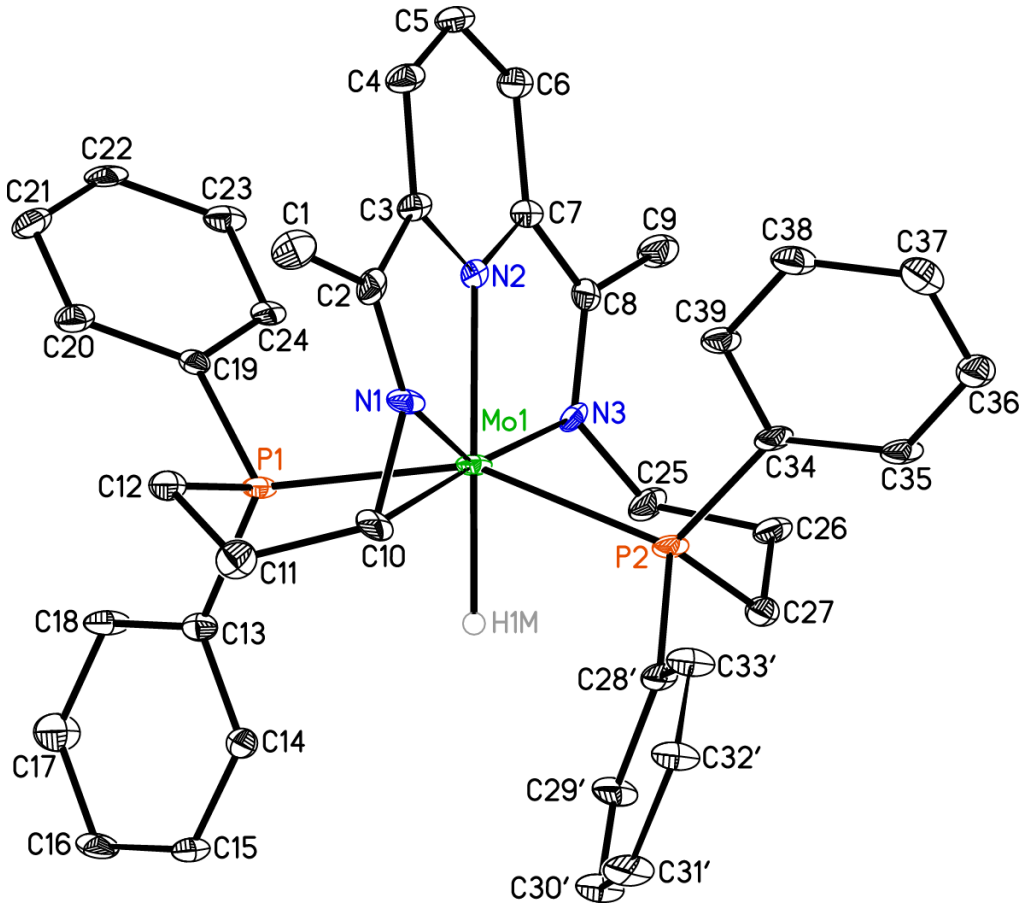

Figure S2. The molecular structure of **(κ^6-*P*,*N*,*N*,*N*,*C*,*P*-^{Ph_2PPr}PDI)MoH** displayed at 30% probability ellipsoids. Hydrogen atoms other than H1M, partially occupied phenyl ring (C28-C33), and partially occupied toluene molecule are omitted for clarity.

Table S3. Metrical parameters for **(κ^6-*P,N,N,N,C,P*-^{Ph_2PPr}PDI)MoH**.

Mo1-N1	1.940(7)	N3-C25	1.469(9)	C20-C21	1.399(10)
Mo1-N2	2.072(5)	C1-C2	1.495(11)	C21-C22	1.374(11)
Mo1-N3	2.121(6)	C2-C3	1.406(10)	C22-C23	1.377(11)
Mo1-C10	2.259(8)	C3-C4	1.401(10)	C23-C24	1.412(10)
Mo1-P2	2.433(2)	C4-C5	1.374(11)	C25-C26	1.547(10)
Mo1-P1	2.448(2)	C5-C6	1.373(11)	C26-C27	1.538(10)
Mo1-H1M	1.75(8)	C6-C7	1.423(9)	C34-C35	1.394(11)
P1-C12	1.831(8)	C7-C8	1.408(11)	C34-C39	1.400(11)
P1-C13	1.834(8)	C8-C9	1.493(11)	C35-C36	1.387(11)
P1-C19	1.840(7)	C10-C11	1.541(11)	C36-C37	1.391(12)
P2-C34	1.824(8)	C11-C12	1.529(10)	C37-C38	1.398(12)
P2-C27	1.829(8)	C13-C18	1.384(11)	C38-C39	1.386(11)
P2-C28'	1.837(4)	C13-C14	1.399(10)	C40-C42	1.382(13)
P2-C28	1.837(4)	C14-C15	1.377(11)	C40-C41	1.402(15)
N1-C2	1.324(9)	C15-C16	1.374(11)	C40-C43	1.61(2)
N1-C10	1.399(9)	C16-C17	1.374(11)	C41-C42	1.395(14)
N2-C7	1.377(9)	C17-C18	1.398(11)	C42-C40	1.382(13)
N2-C3	1.417(9)	C19-C24	1.370(10)		
N3-C8	1.374(9)	C19-C20	1.391(10)		

N1-Mo1-N2	72.4(2)	C34-P2-C28	100.2(3)	N1-C10-C11	117.6(7)
N1-Mo1-N3	144.3(2)	C27-P2-C28	101.5(3)	N1-C10-Mo1	58.5(4)
N2-Mo1-N3	72.9(2)	C34-P2-Mo1	116.8(2)	C11-C10-Mo1	121.4(5)
N1-Mo1-C10	38.0(2)	C27-P2-Mo1	112.1(3)	C12-C11-C10	110.8(6)
N2-Mo1-C10	109.8(3)	C28'-P2-Mo1	115.1(2)	C11-C12-P1	108.5(5)
N3-Mo1-C10	176.8(3)	C28-P2-Mo1	119.3(2)	C18-C13-C14	118.0(7)
N1-Mo1-P2	100.84(19)	C2-N1-C10	143.2(7)	C18-C13-P1	122.3(5)
N2-Mo1-P2	112.10(16)	C2-N1-Mo1	127.5(5)	C14-C13-P1	119.6(6)
N3-Mo1-P2	84.56(16)	C10-N1-Mo1	83.5(4)	C15-C14-C13	120.9(8)
C10-Mo1-P2	92.7(2)	C7-N2-C3	120.8(6)	C16-C15-C14	121.2(7)
N1-Mo1-P1	86.41(19)	C7-N2-Mo1	121.4(5)	C17-C16-C15	118.4(7)
N2-Mo1-P1	94.98(16)	C3-N2-Mo1	117.8(5)	C16-C17-C18	121.4(8)
N3-Mo1-P1	104.79(17)	C8-N3-C25	115.7(6)	C13-C18-C17	120.1(7)
C10-Mo1-P1	77.0(2)	C8-N3-Mo1	119.2(5)	C24-C19-C20	119.9(7)
P2-Mo1-P1	152.91(7)	C25-N3-Mo1	124.5(5)	C24-C19-P1	117.3(5)
N1-Mo1-H1M	122.(3)	N1-C2-C3	109.9(7)	C20-C19-P1	122.8(6)
N2-Mo1-H1M	165.(3)	N1-C2-C1	124.3(7)	C19-C20-C21	119.3(8)
N3-Mo1-H1M	94.(3)	C3-C2-C1	125.8(7)	C22-C21-C20	120.3(8)
C10-Mo1-H1M	84.(3)	C4-C3-C2	130.2(7)	C21-C22-C23	121.2(7)
P2-Mo1-H1M	73.(3)	C4-C3-N2	118.7(7)	C22-C23-C24	118.3(8)
P1-Mo1-H1M	81.(3)	C2-C3-N2	111.2(6)	C19-C24-C23	121.1(7)
C12-P1-C13	101.0(3)	C5-C4-C3	120.1(8)	N3-C25-C26	110.8(7)
C12-P1-C19	104.5(3)	C6-C5-C4	121.9(7)	C27-C26-C25	113.9(7)
C13-P1-C19	103.0(3)	C5-C6-C7	119.2(7)	C26-C27-P2	115.7(5)
C12-P1-Mo1	104.9(3)	N2-C7-C8	112.6(6)	C29-C28-P2	118.0(3)
C13-P1-Mo1	123.5(3)	N2-C7-C6	119.4(7)	C33-C28-P2	124.0(2)
C19-P1-Mo1	117.3(2)	C8-C7-C6	127.9(7)	C29'-C28'-P2	121.3(3)
C34-P2-C27	104.9(4)	N3-C8-C7	113.7(7)	C33'-C28'-P2	120.8(3)
C34-P2-C28'	103.9(3)	N3-C8-C9	123.4(7)	C35-C34-C39	118.1(7)
C27-P2-C28'	102.6(3)	C7-C8-C9	122.9(6)	C35-C34-P2	123.8(6)

C39-C34-P2	118.0(6)	C39-C38-C37	120.2(8)	C41-C40-C43	125.5(11)
C36-C35-C34	121.6(8)	C38-C39-C34	120.9(8)	C42-C41-C40	122.8(9)
C35-C36-C37	119.8(8)	C42-C40-C41	118.9(10)	C40-C42-C41	118.3(10)
C36-C37-C38	119.4(8)	C42-C40-C43	115.6(12)		

NMR and IR Spectroscopic Data Recorded for Newly Prepared Complexes:

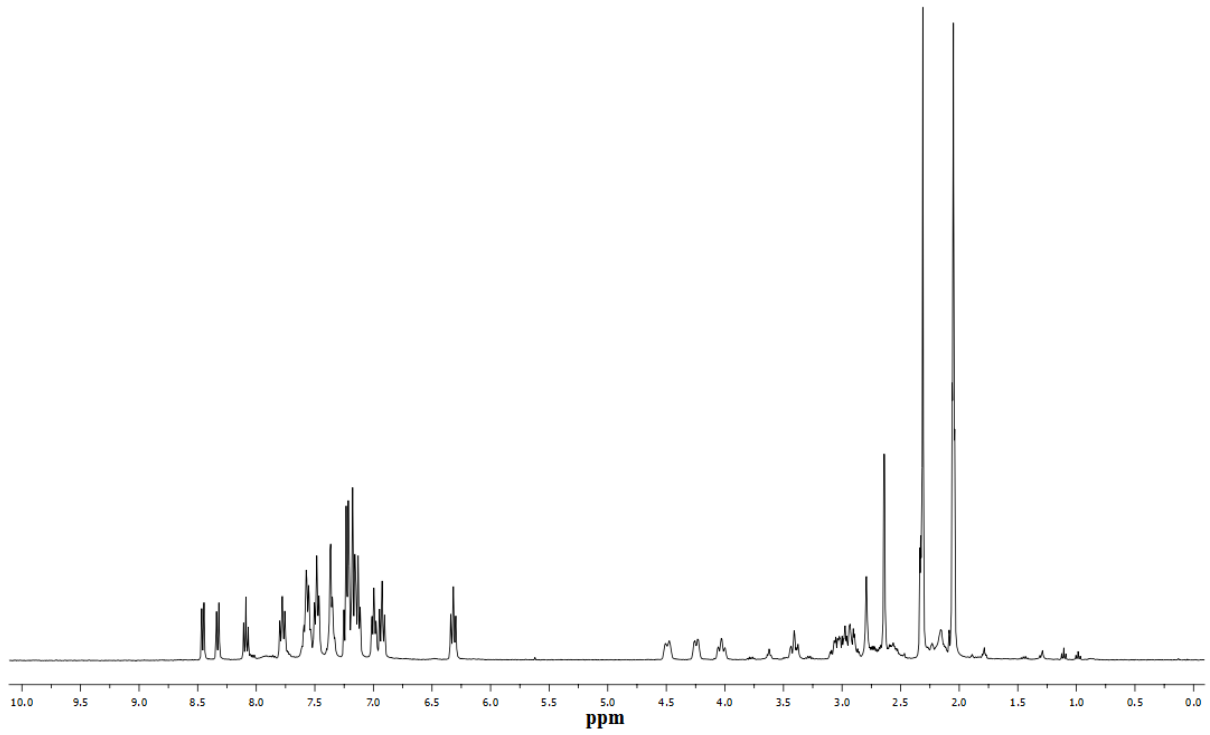

Figure S3. ^{1}H NMR spectrum of **[(^{Ph_2PPr}PDI)MoI(CO)][I]** in acetone-d_6.

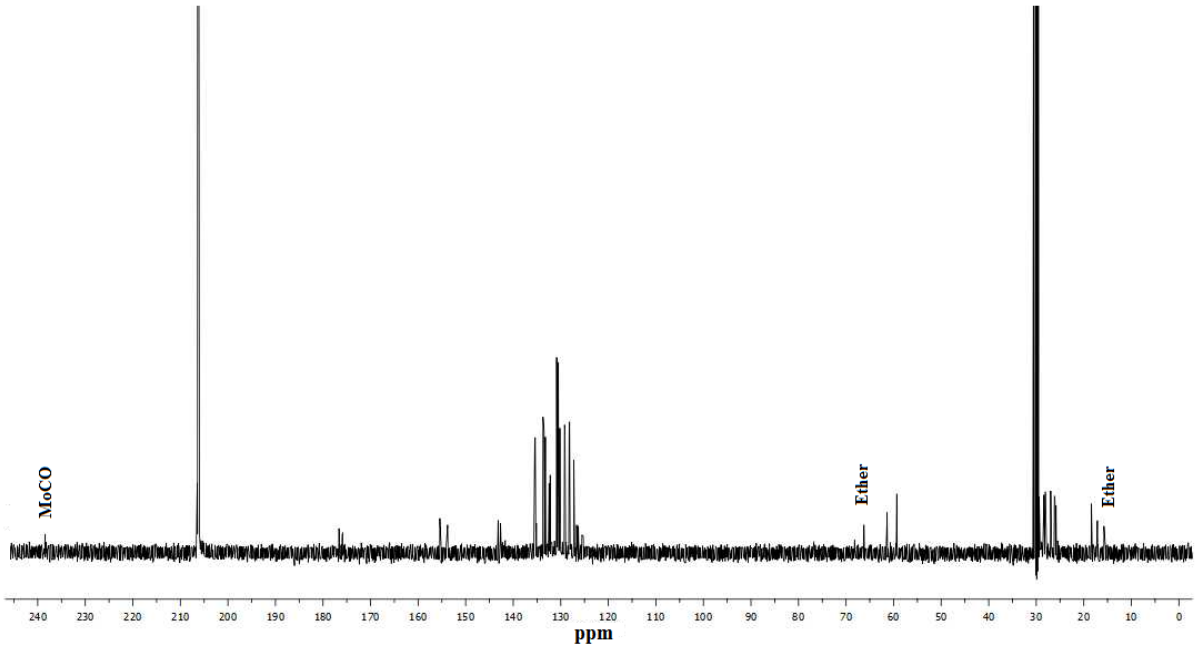

Figure S4. ^{13}C NMR spectrum of **[(**^{Ph_2PPr}**PDI)MoI(CO)][I]** in acetone-d_6.

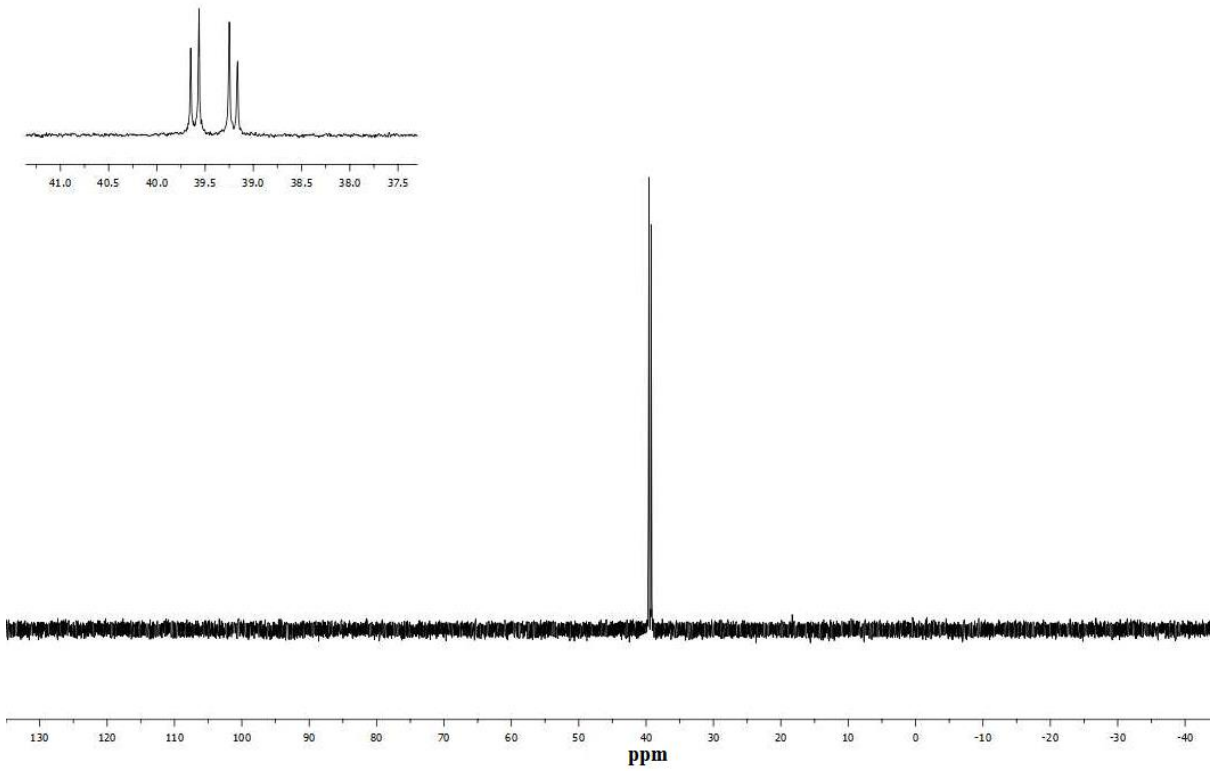

Figure S5. ^{31}P NMR spectrum of **[(**^{Ph_2PPr}**PDI)MoI(CO)][I]** in acetone-d_6.

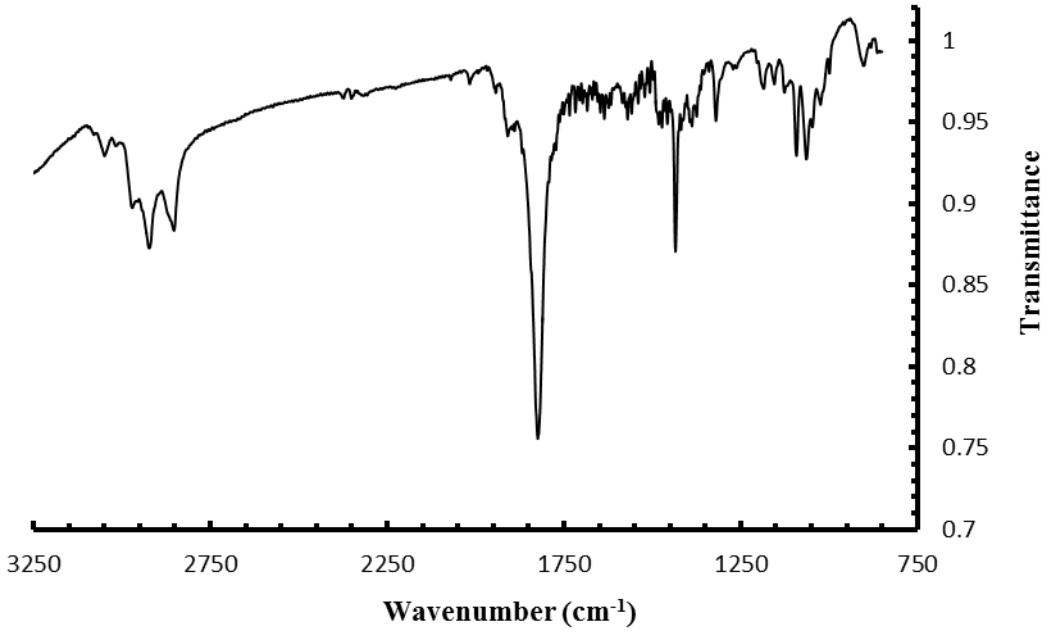

Figure S6. Infrared spectrum of **[(^{Ph_2PPr}PDI)MoI(CO)][I]** in KBr.

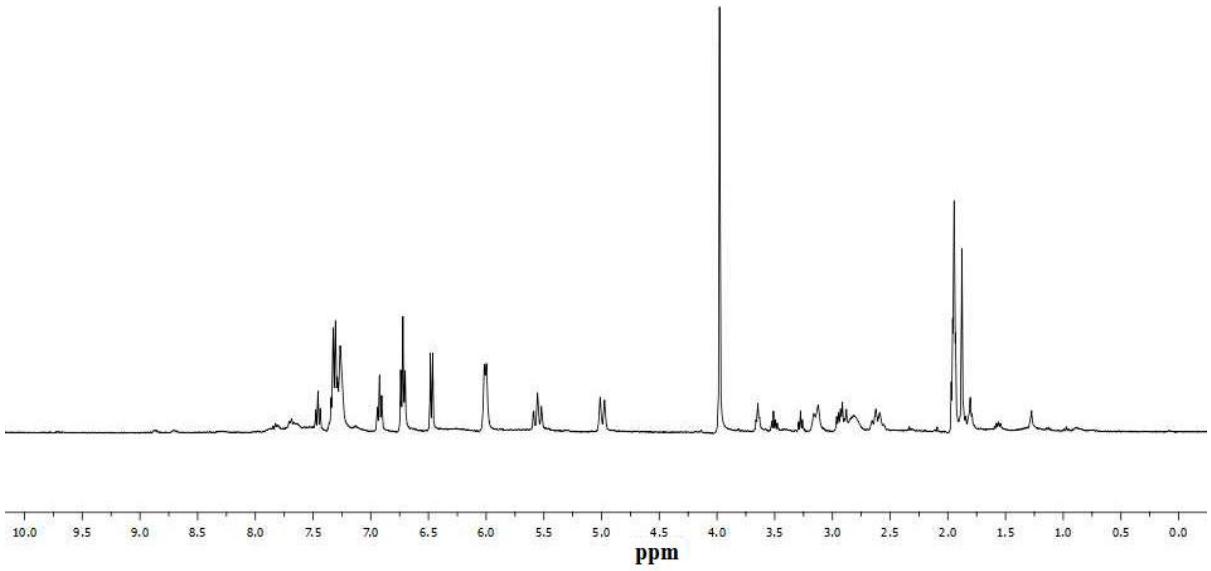

Figure S7. ^{1}H NMR spectrum of **[(^{Ph_2PPr}PDI)MoI][I]** in acetonitrile-d_3.

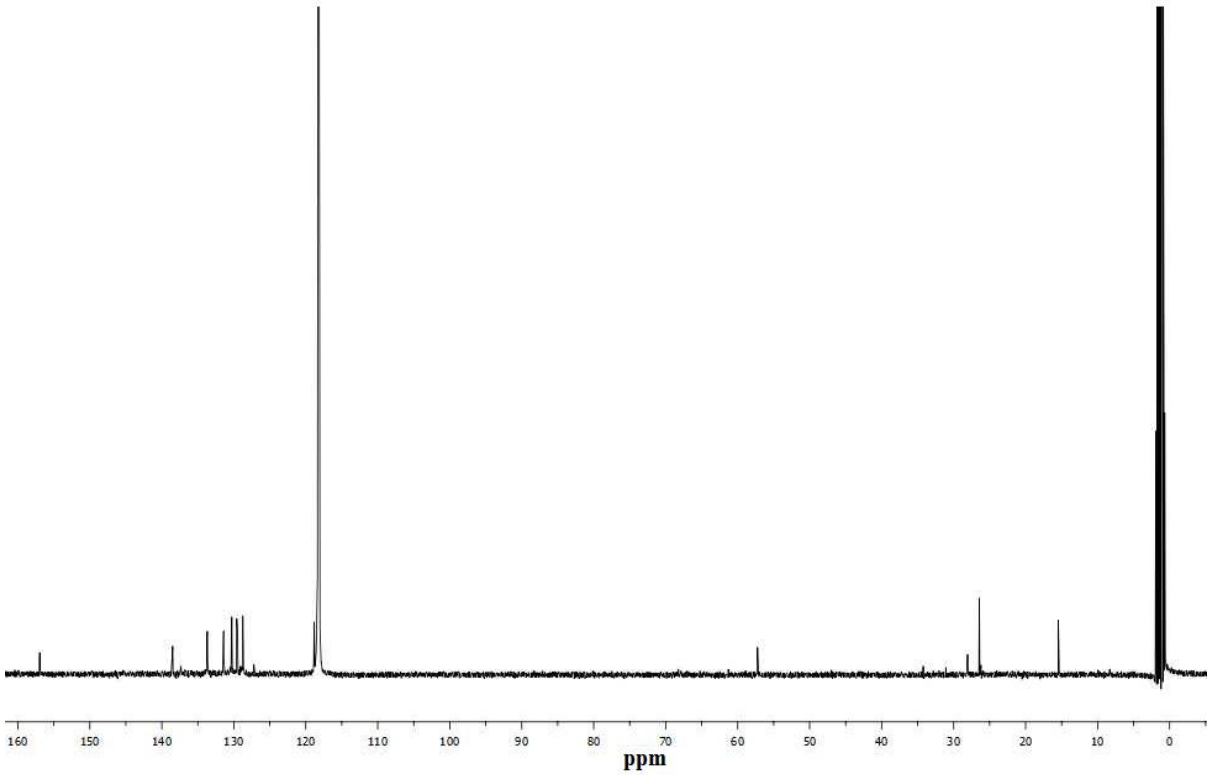

Figure S8. ^{13}C NMR spectrum of **[(**^{Ph_2PPr}**PDI)MoI][I]** in acetonitrile-d_3.

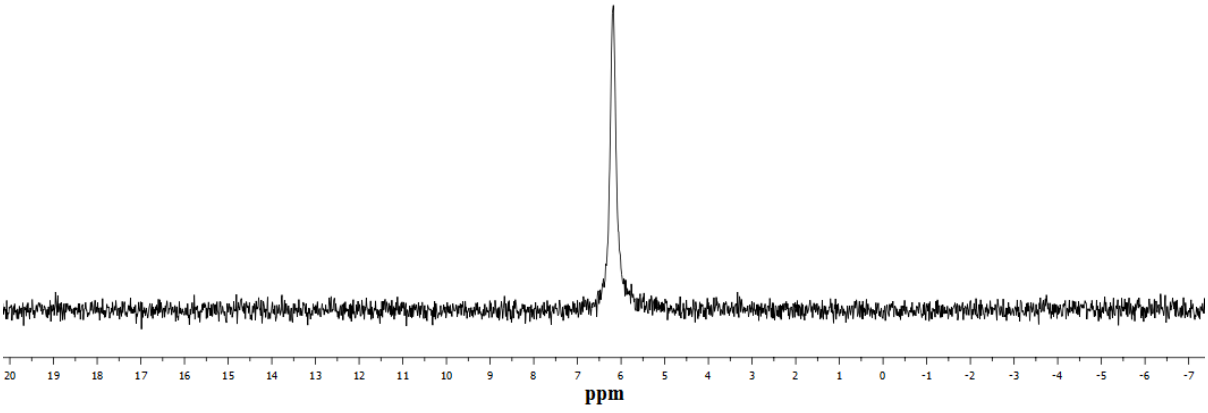

Figure S9. ^{31}P NMR spectrum of **[(**^{Ph_2PPr}**PDI)MoI][I]** in acetonitrile-d_3.

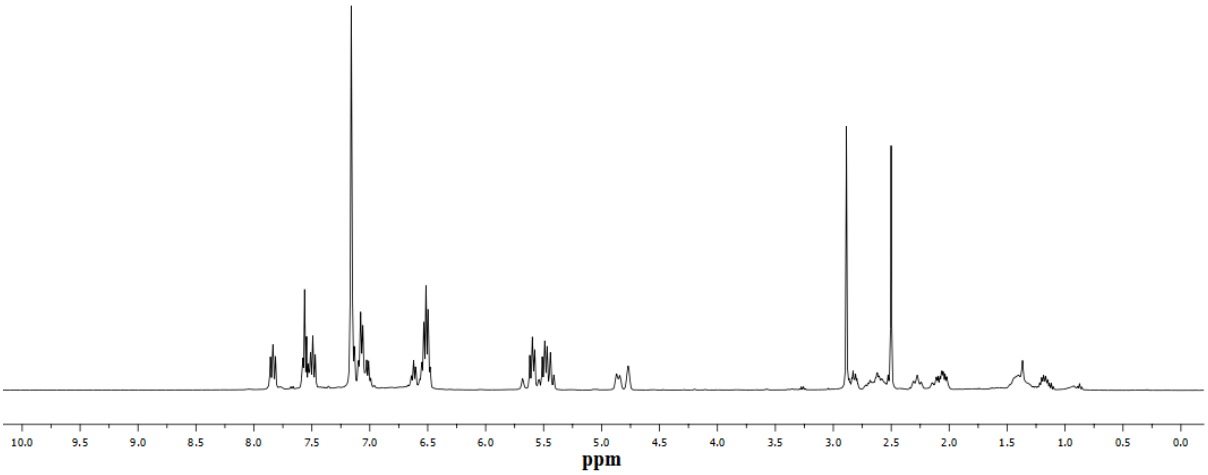

Figure S10. ^{1}H NMR spectrum of **(κ^{6}-*P,N,N,N,C,P*-^{Ph_2PPr}PDI)MoH** in benzene-d_6.

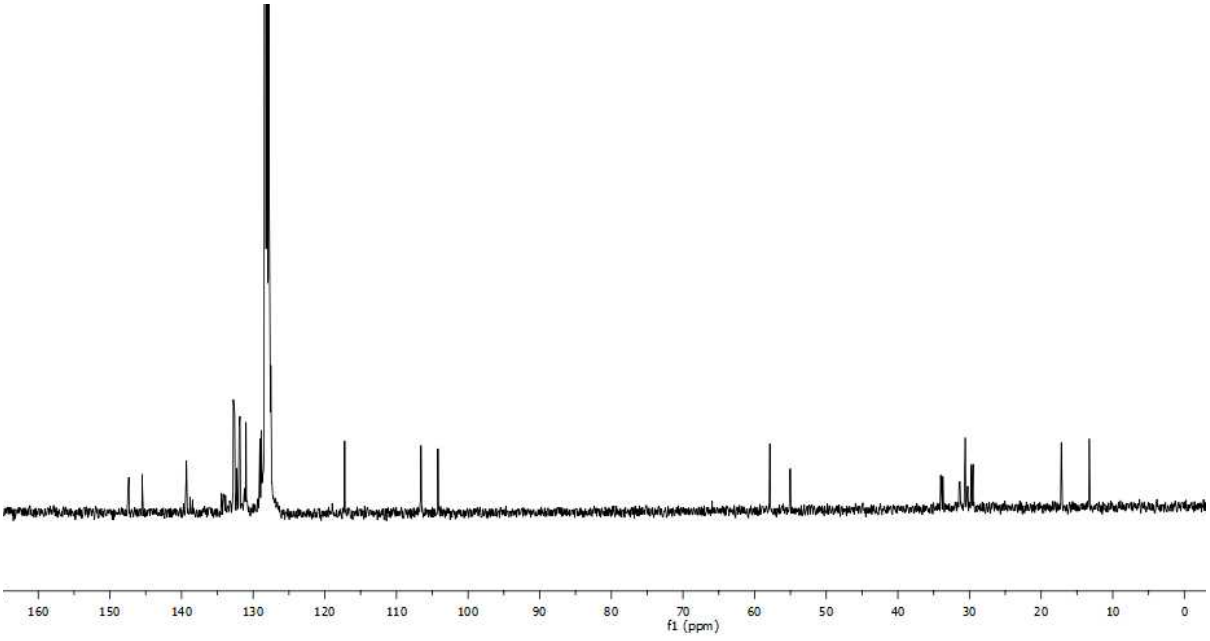

Figure S11. ^{13}C NMR spectrum of **(κ^{6}-*P,N,N,N,C,P*-^{Ph_2PPr}PDI)MoH** in benzene-d_6

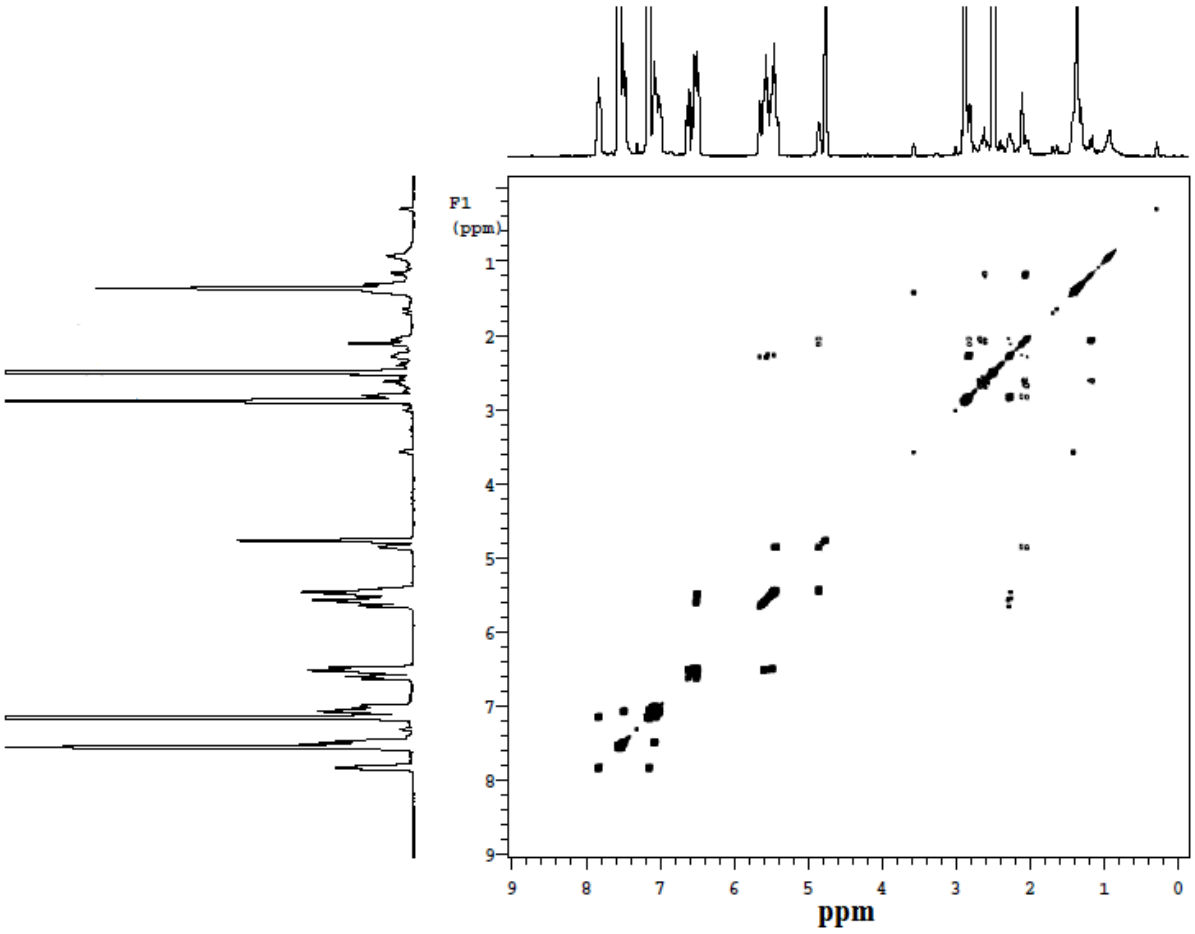

Figure S12. gCOSY NMR spectrum of **(κ^6-*P*,*N*,*N*,*N*,*C*,*P*-^{Ph_2PPr}PDI)MoH** in benzene-d_6.

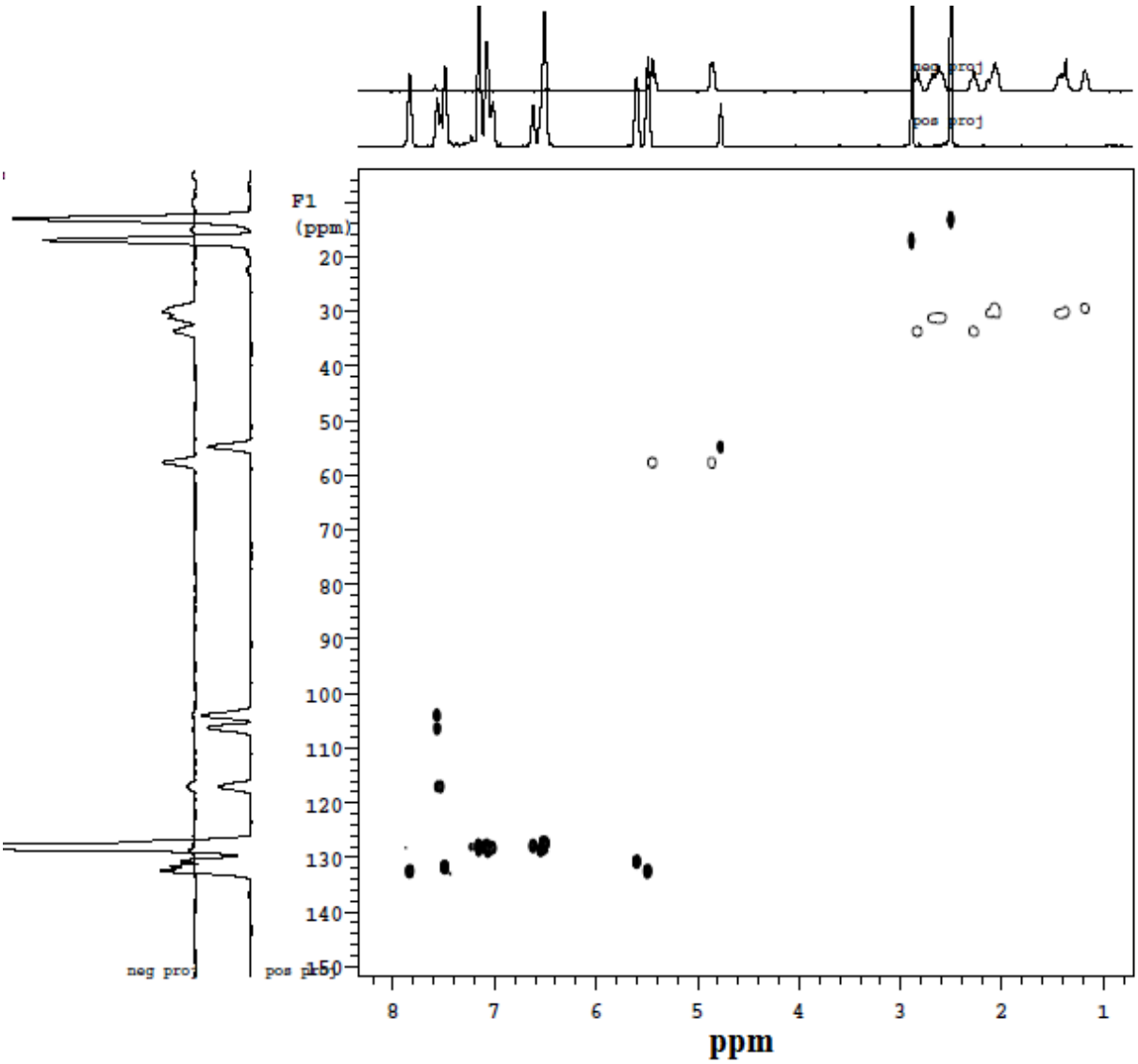

Figure S13. gHSQCAD NMR spectrum of **(κ^6-*P*,*N*,*N*,*N*,*C*,*P*-^{Ph_2PPr}PDI)MoH** in benzene-d_6.

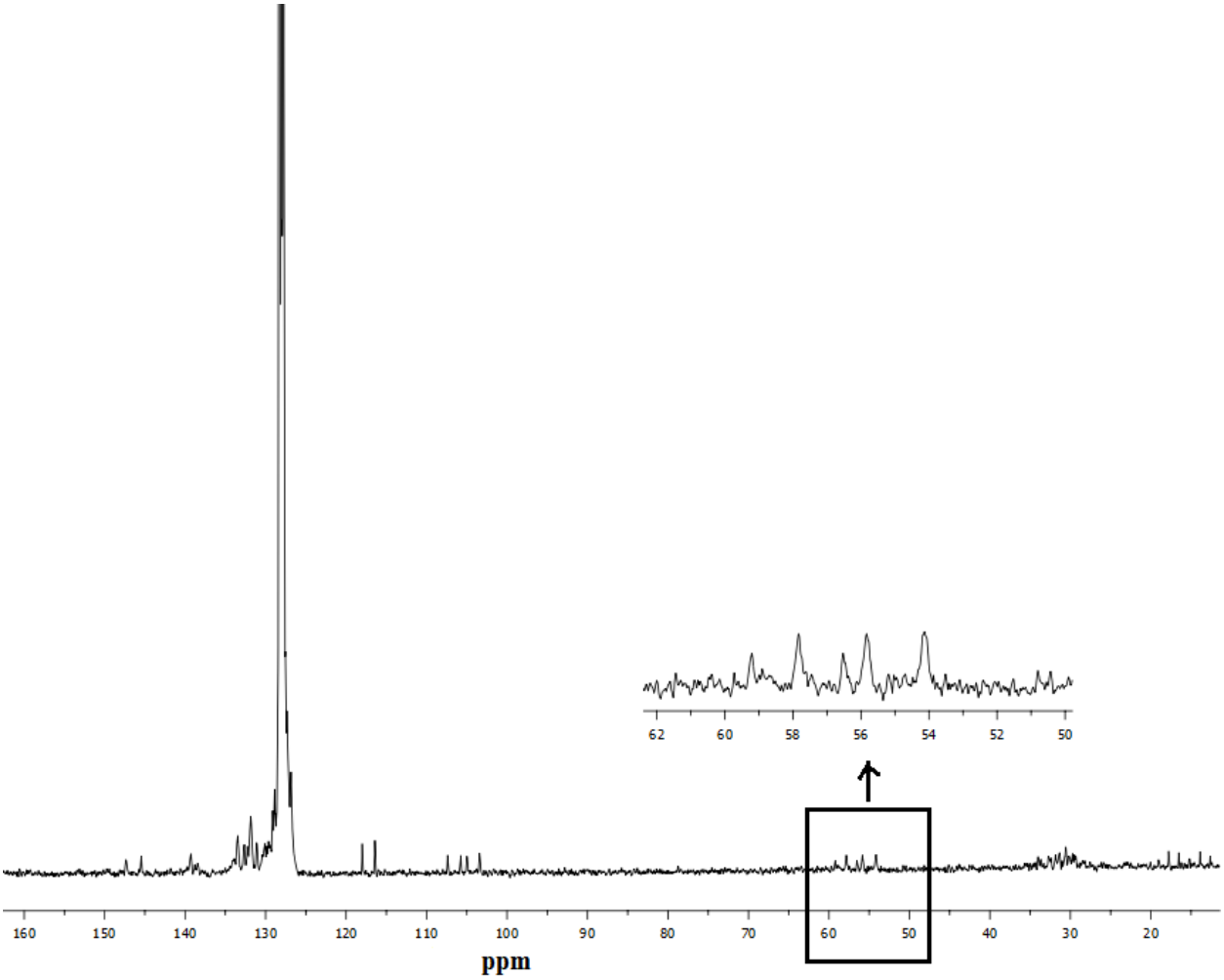

Figure S14. ^{1}H-coupled ^{13}C NMR spectrum of **(κ^{6}-*P*,*N*,*N*,*N*,*C*,*P*-^{Ph_2PPr}PDI)MoH** in benzene-d_6.

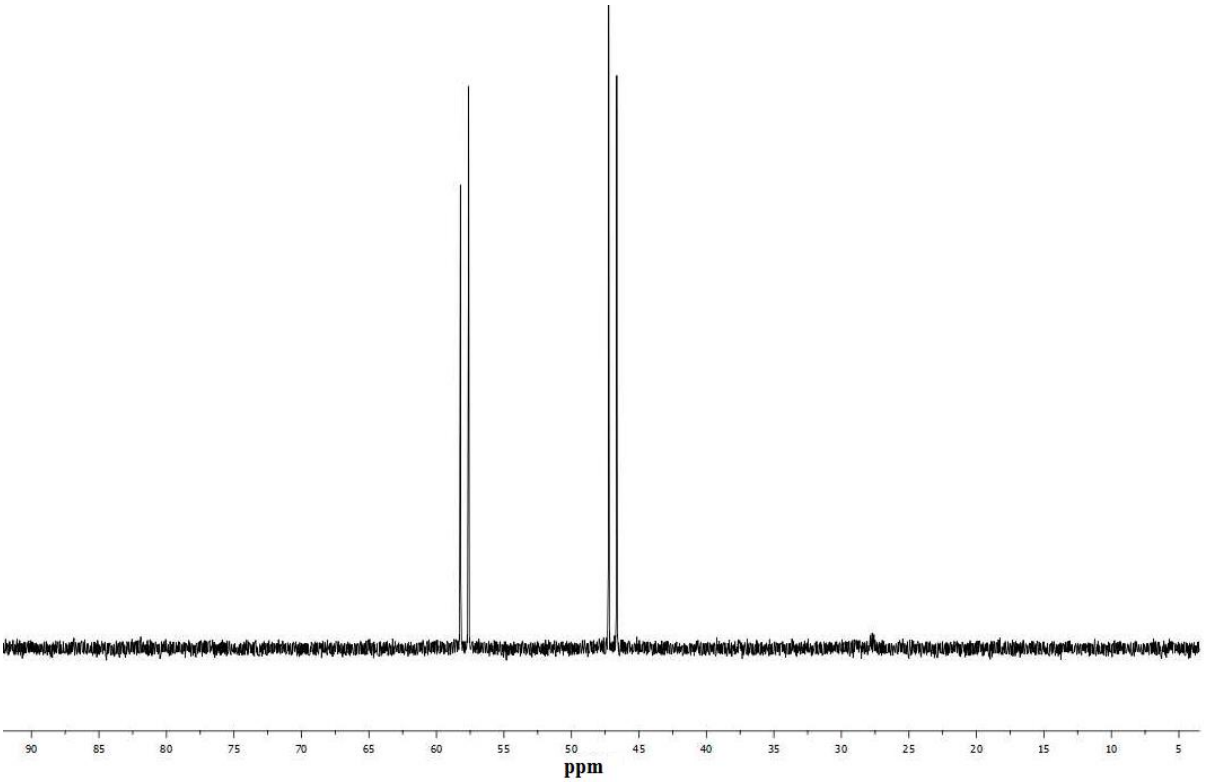

Figure S15. ^{31}P NMR spectrum of **(κ^6-*P,N,N,N,C,P*-^{Ph_2PPr}PDI)MoH** in benzene-d_6.

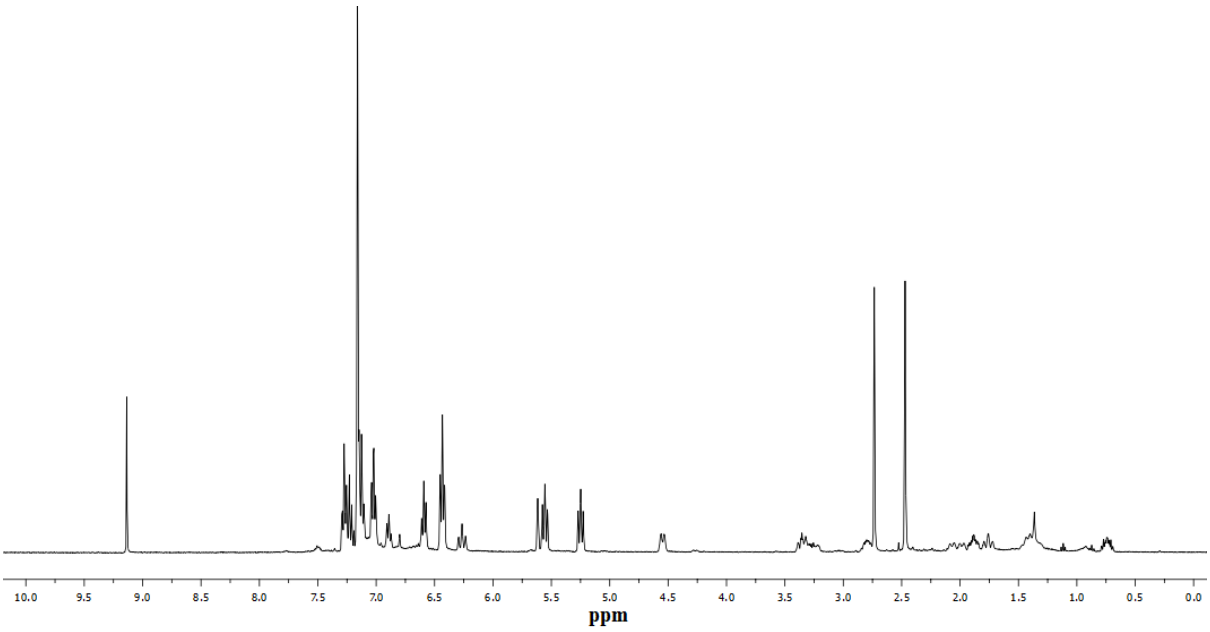

Figure S16. ^{1}H NMR spectrum of **(κ^6-*P,N,N,N,C,P*-^{Ph_2PPr}PDI)Mo(OCOH)** in benzene-d_6.

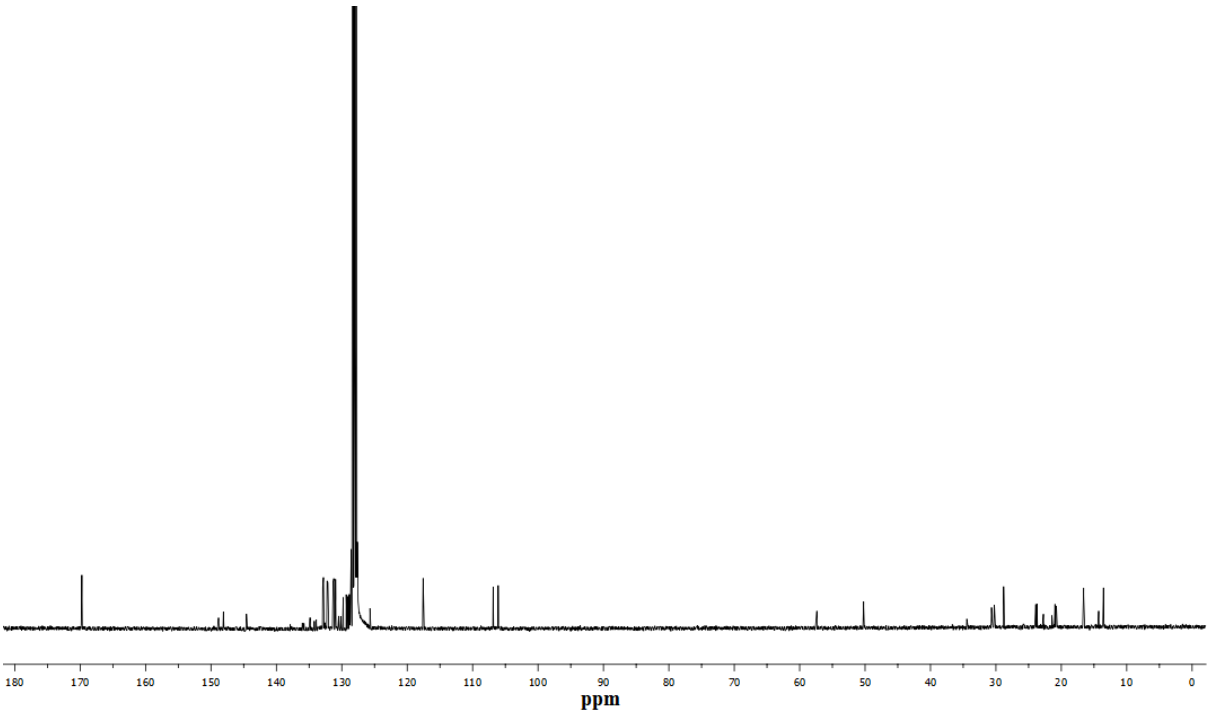

Figure S17. ^{13}C NMR spectrum of **(κ^6-*P*,*N*,*N*,*N*,*C*,*P*-^{Ph_2PPr}PDI)Mo(OCOH)** in benzene-d_6.

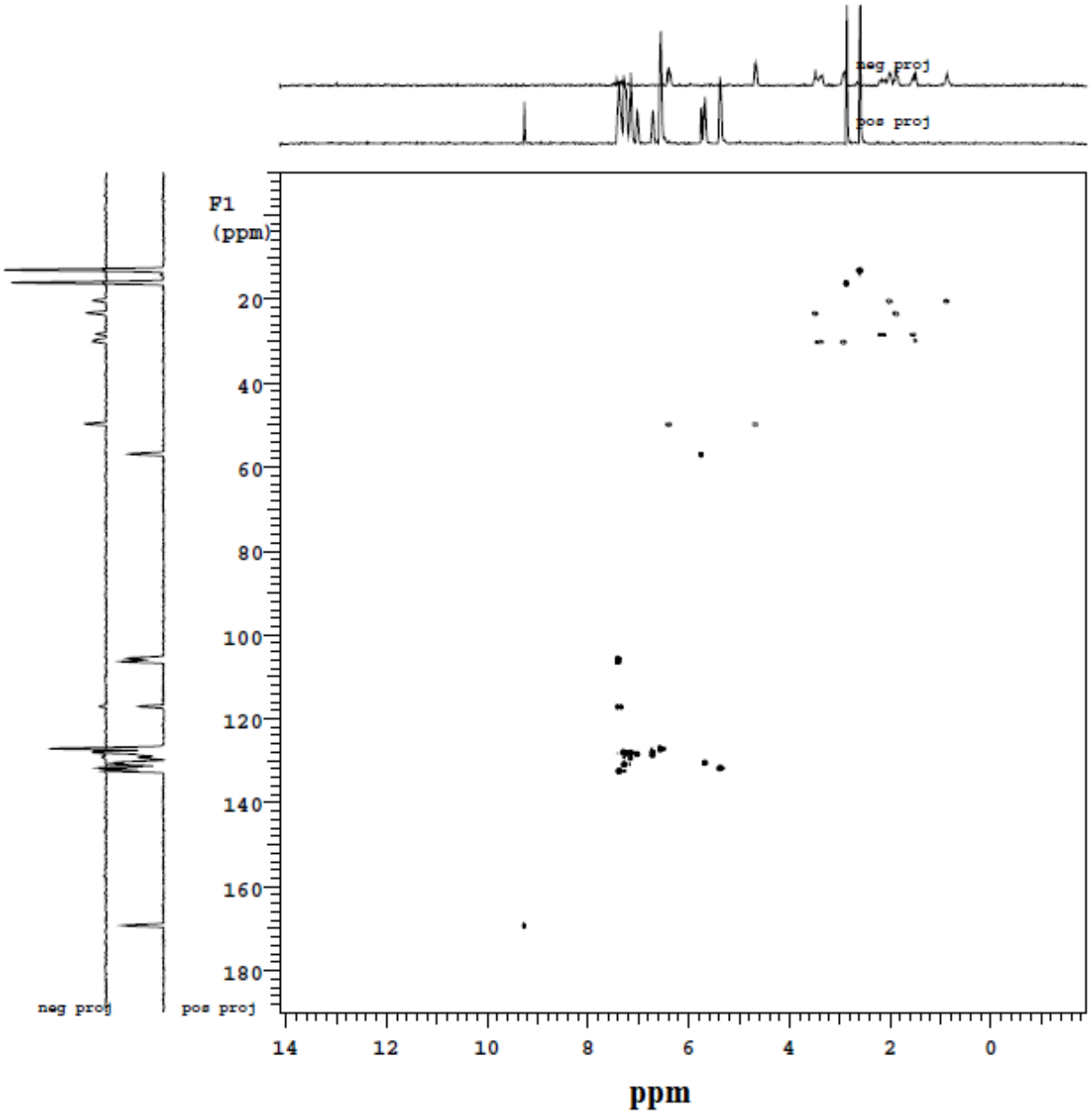

Figure S18. gHSQCAD NMR spectrum of **(κ^6-*P*,*N*,*N*,*N*,*C*,*P*-^{Ph_2PPr}PDI)Mo(OCOH)** in benzene-d_6.

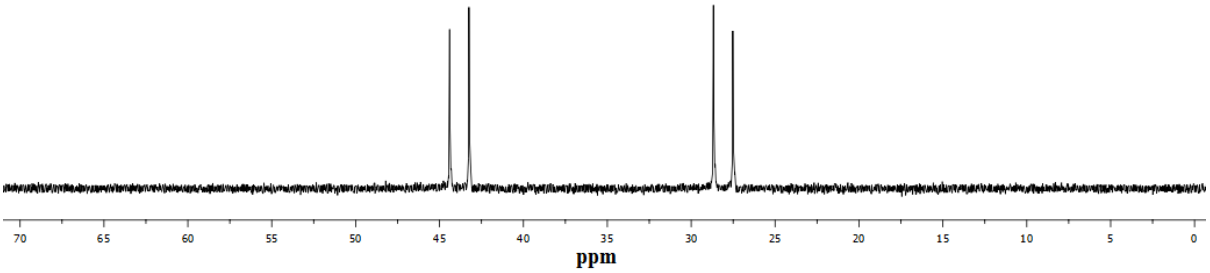

Figure S19. ^{31}P NMR spectrum of **(κ^6-*P,N,N,N,C,P*-^{Ph_2PPr}PDI)Mo(OCOH)** in benzene-d_6.

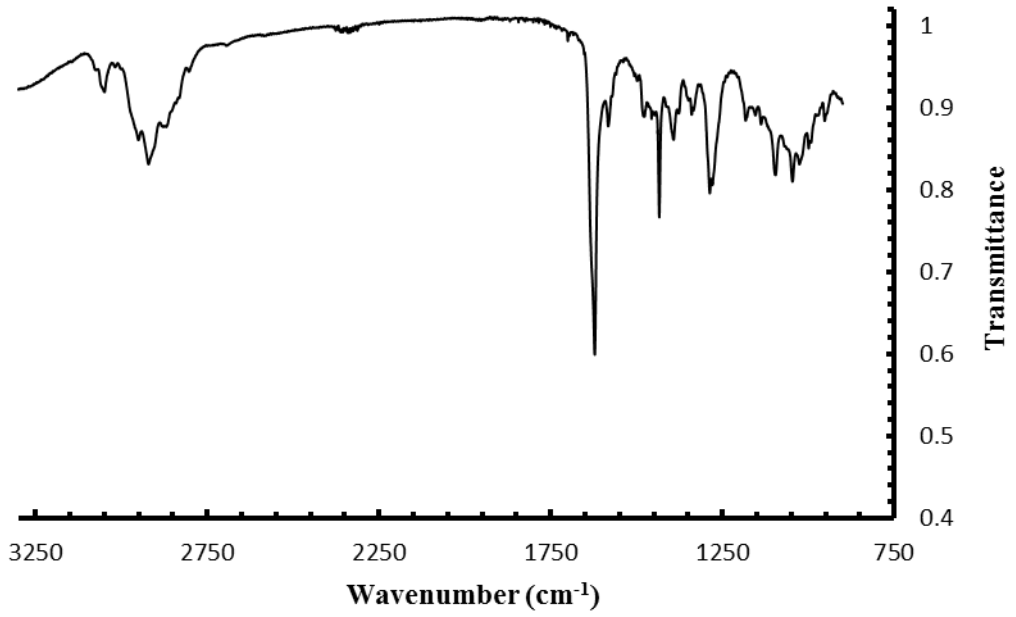

Figure S20. Infrared spectrum of **(κ^6-*P,N,N,N,C,P*-^{Ph_2PPr}PDI)Mo(OCOH)** in KBr.

Supporting Data for CO_2 Reduction Experiments:

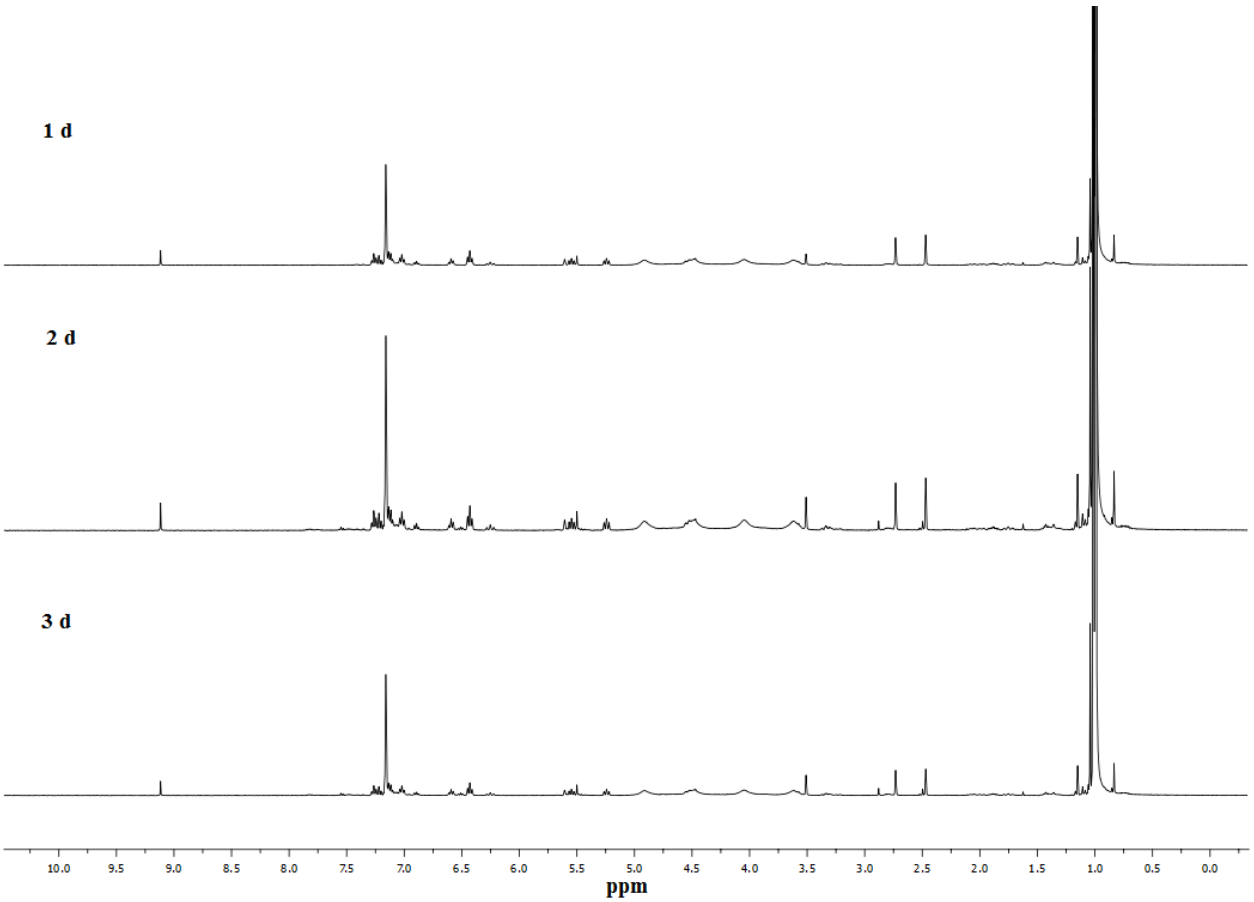

Figure S21. ^{1}H NMR spectra illustrating the slow conversion of CO_2 to $H_3COBPin$ and $O(BPin)_2$ over 3 d at 25 °C using **(κ^6-*P,N,N,N,C,P*-^{Ph_2PPr}PDI)MoH**.

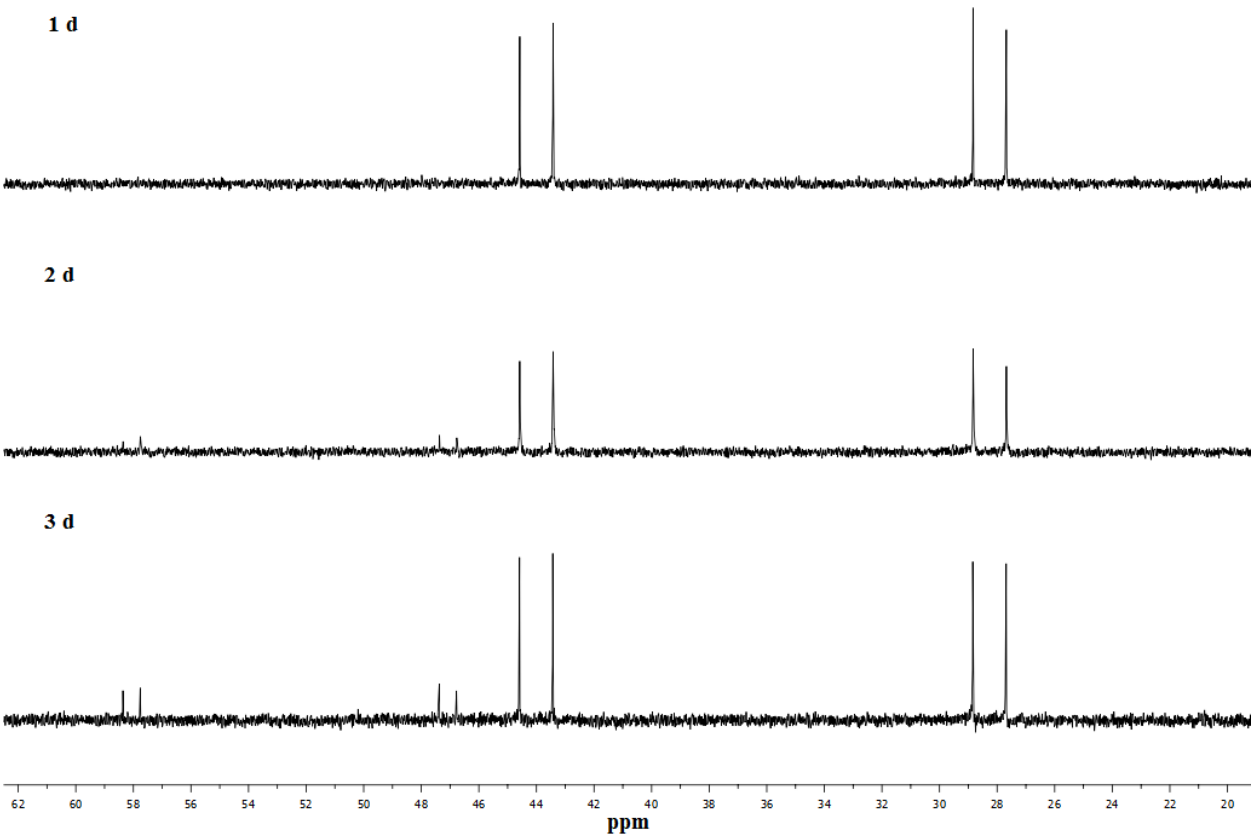

Figure S22. ^{31}P NMR spectra illustrating the partial conversion of **(κ^6-*P*,*N*,*N*,*N*,*C*,*P*-^{Ph_2PPr}PDI)Mo(OCOH)** to **(κ^6-*P*,*N*,*N*,*N*,*C*,*P*-^{Ph_2PPr}PDI)MoH** over 3 d at 25 °C.

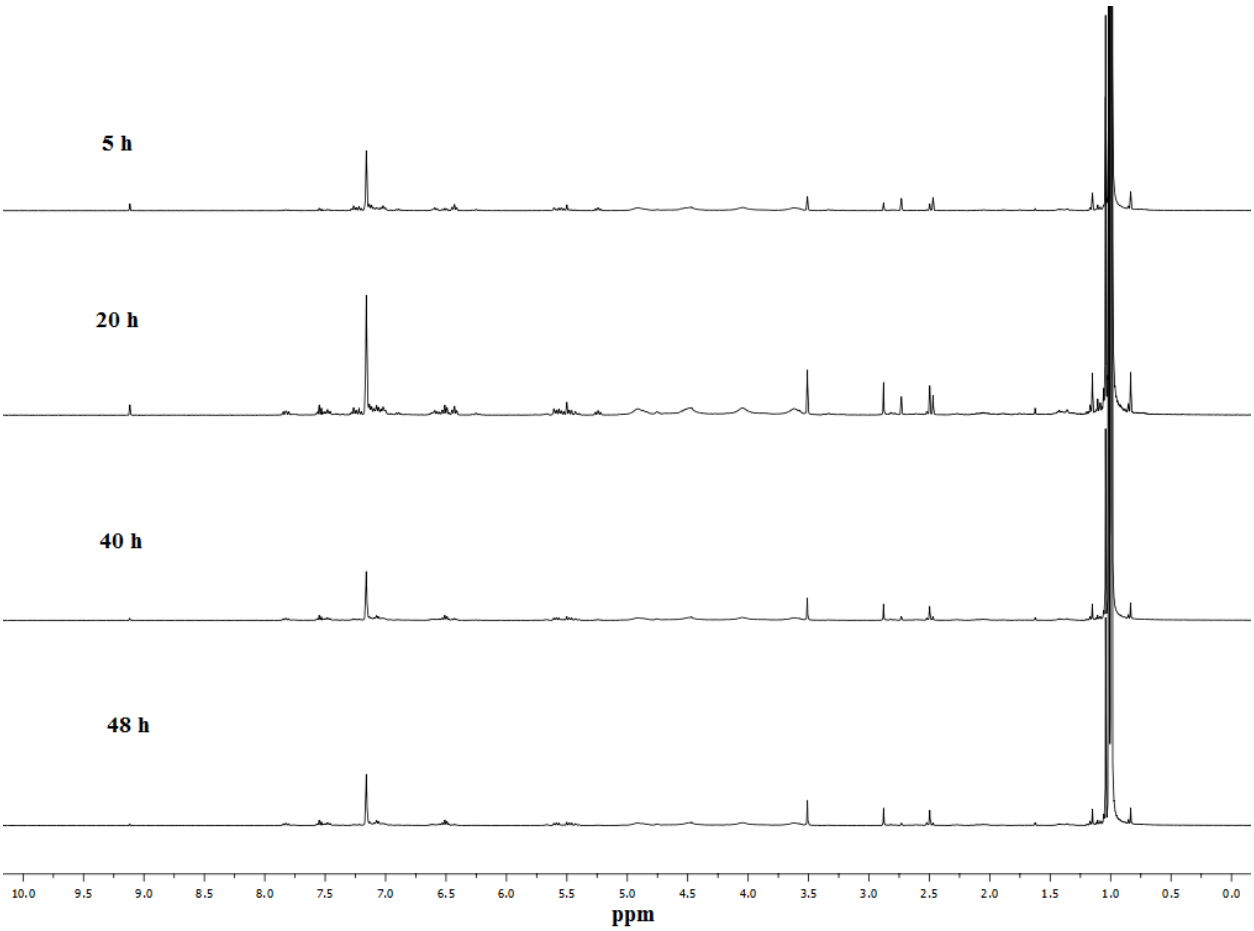

Figure S23. ^{1}H NMR spectra illustrating the stoichiometric conversion of CO_2 to $H_3COBPin$ and $O(BPin)_2$ over 2 d at 60 °C using **(κ^{6}-*P*,*N*,*N*,*N*,*C*,*P*-^{Ph_2PPr}PDI)MoH**.

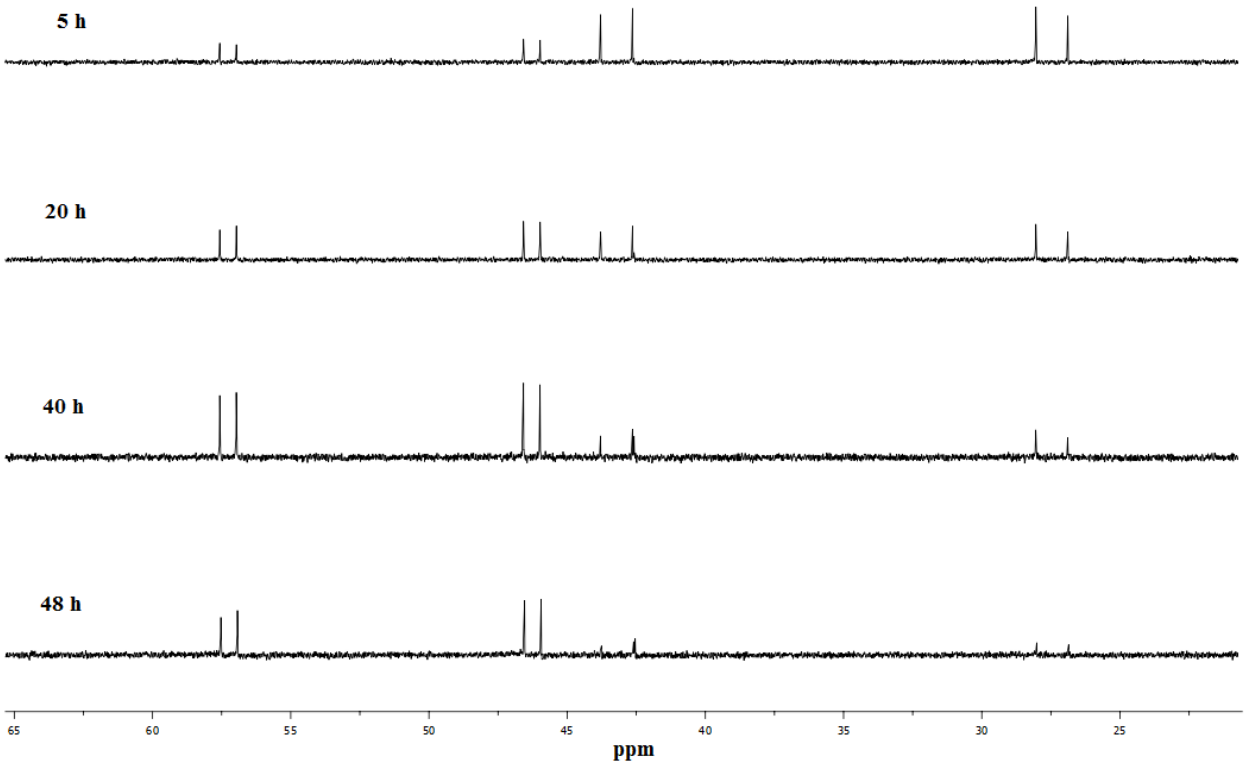

Figure S24. ^{31}P NMR spectra illustrating the conversion of **(κ^6-*P,N,N,N,C,P*-^{Ph_2PPr}PDI)Mo(OCOH)** to **(κ^6-*P,N,N,N,C,P*-^{Ph_2PPr}PDI)MoH** over 2 d at 60 °C.

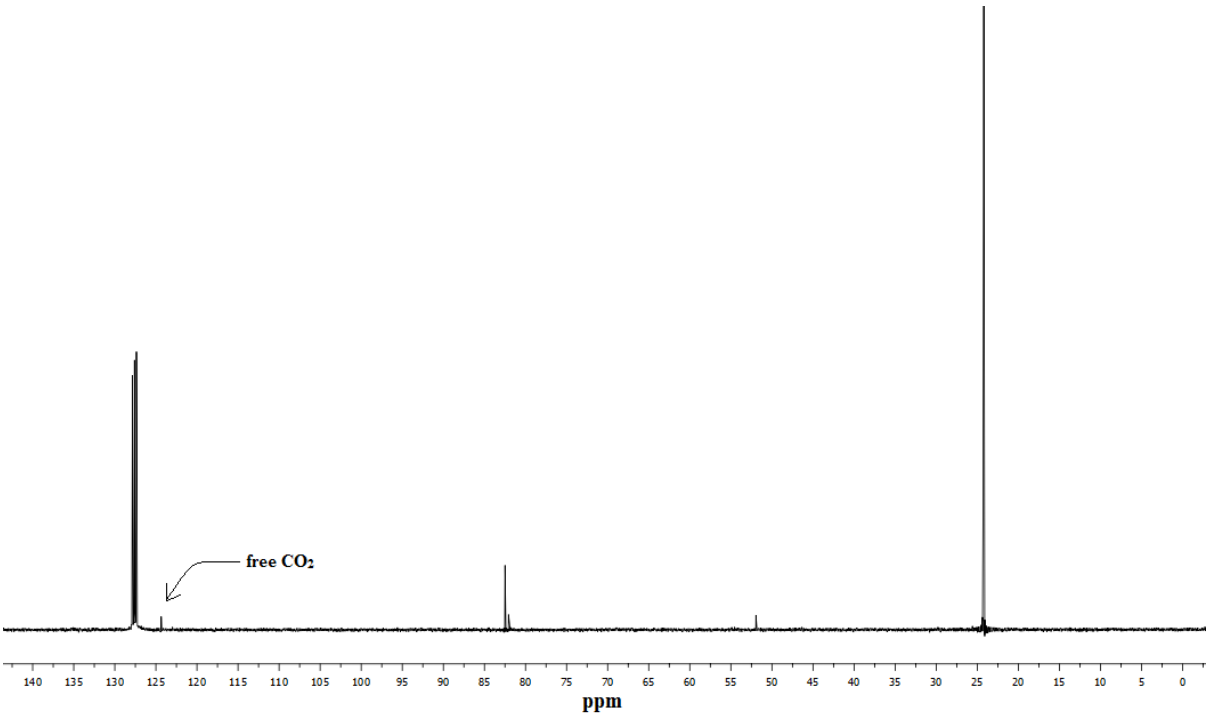

Figure S25. ^{13}C NMR spectrum of CO_2 hydroboration using 1 mol% **(κ^6-*P,N,N,N,C,P*-^{Ph_2PPr}PDI)MoH** after 5 h at 90 °C in benzene-d_6.

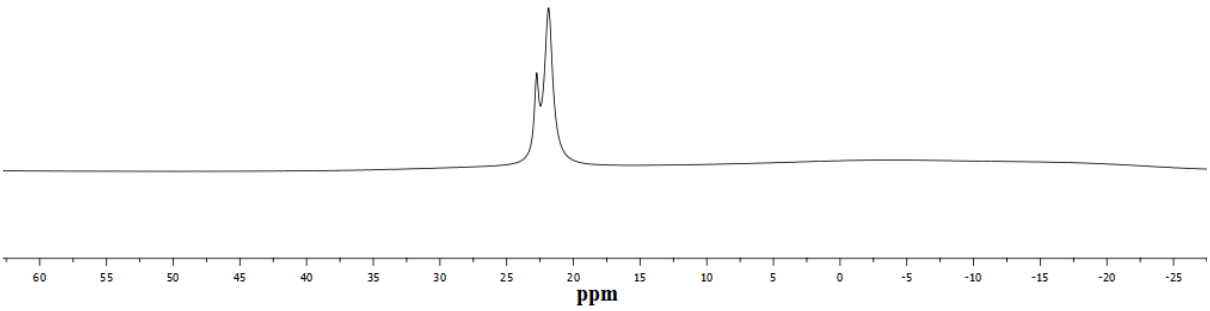

Figure S26. ^{11}B NMR spectrum of CO_2 hydroboration using 1 mol% **(κ^6-*P,N,N,N,C,P*-^{Ph_2PPr}PDI)MoH** after 5 h at 90 °C in benzene-d_6.

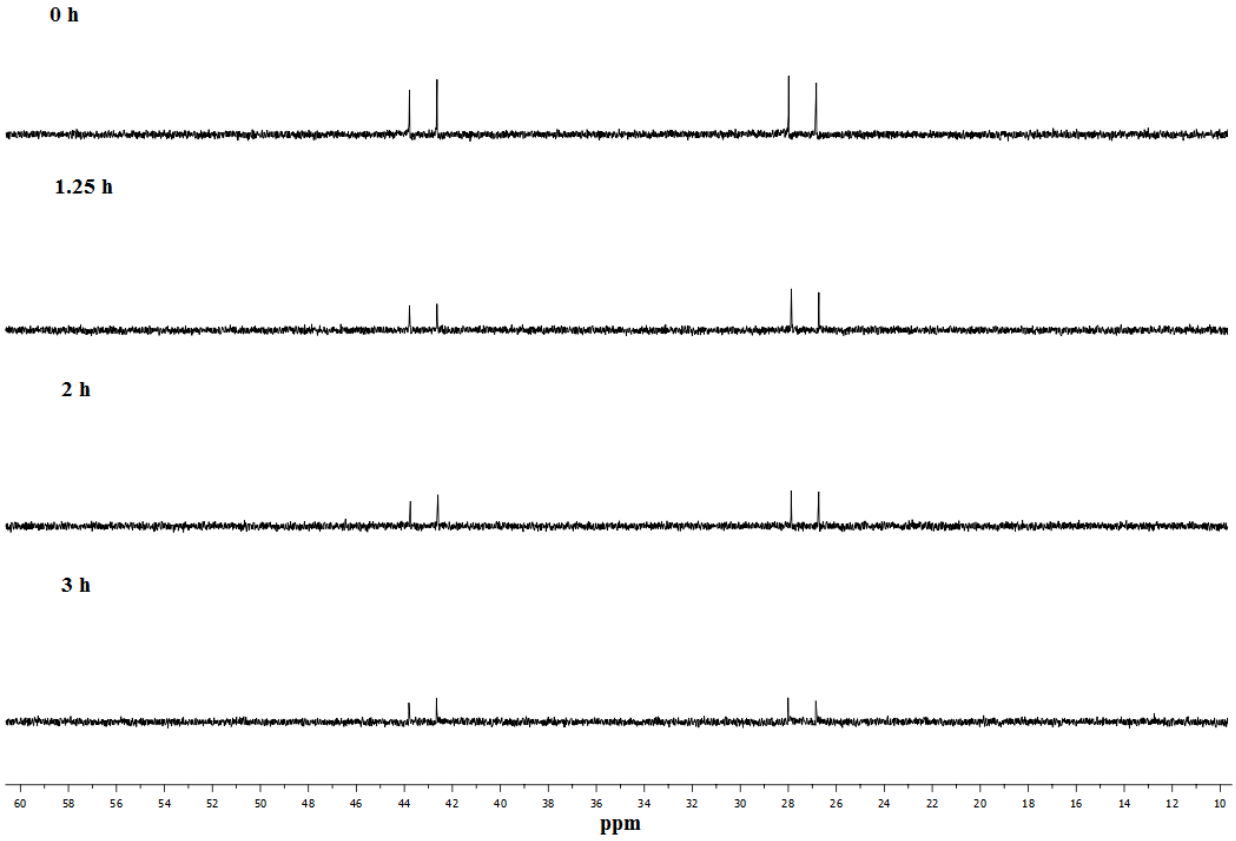

Figure S27. Observation of **5** by ^{31}P NMR spectroscopy during CO_2 hydroboration.

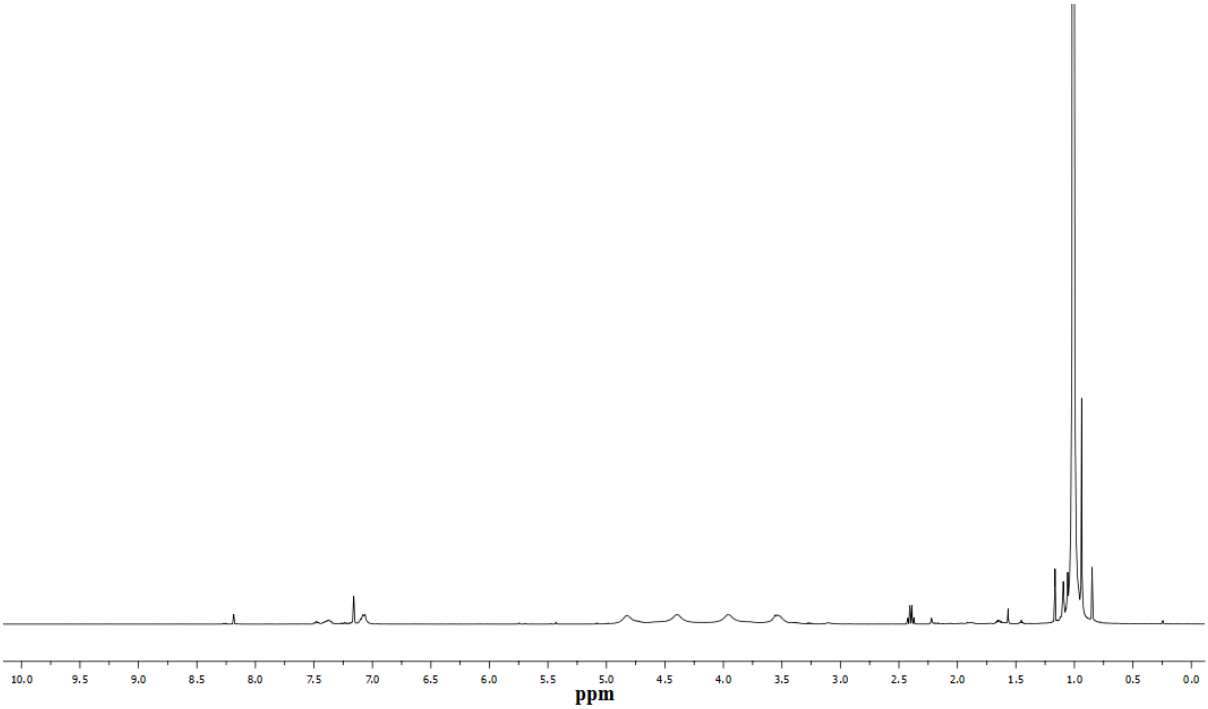

Figure S28. ^{1}H NMR spectrum of attempted CO_2 hydroboration using 1.0 mol% ^{Ph_2PPr}**PDI** as a catalyst (benzene-d_6).

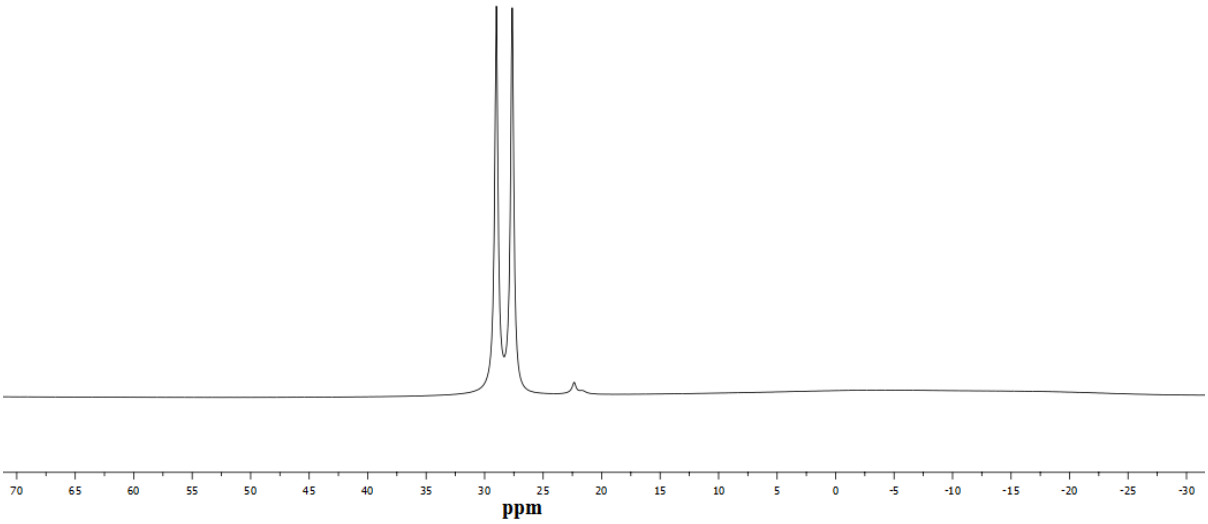

Figure S29. ^{11}B NMR spectrum of attempted CO_2 hydroboration using 1.0 mol% ^{Ph_2PPr}**PDI** as a catalyst (benzene-d_6).

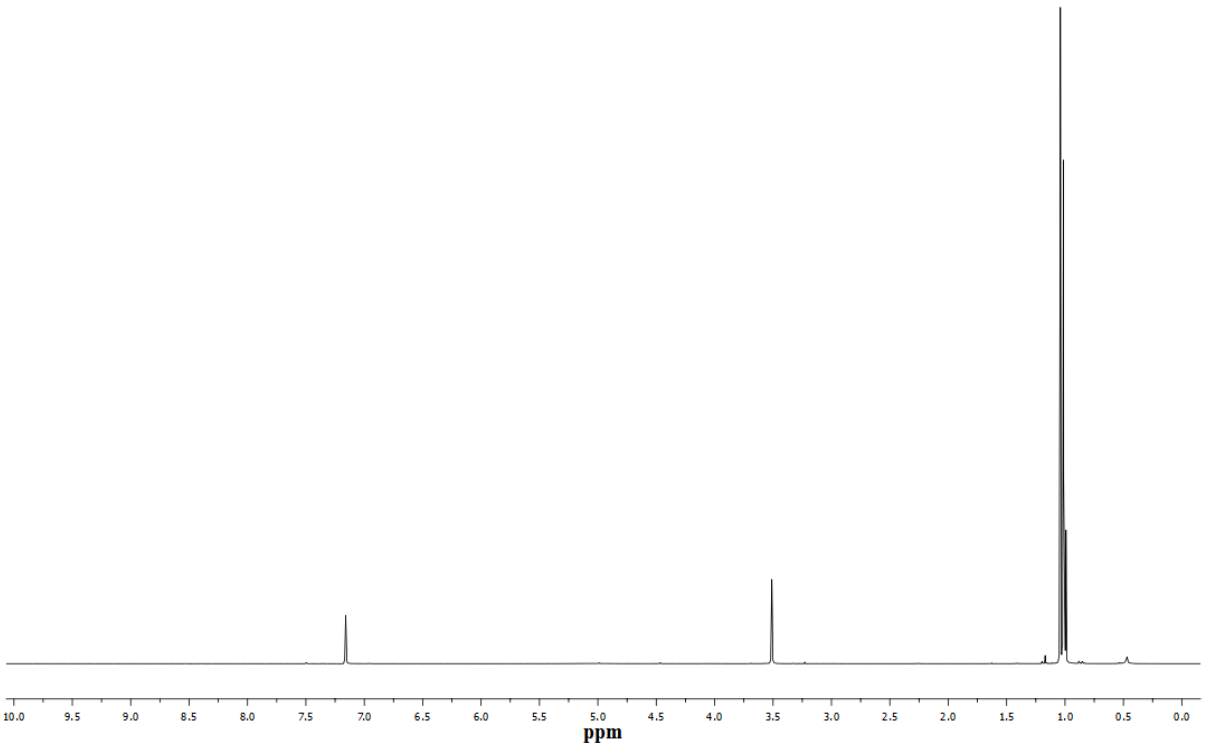

Figure S30. ^{1}H NMR spectrum of CO_2 hydroboration using 0.1 mol% **(κ^{6}-*P,N,N,N,C,P*-^{Ph_2PPr}PDI)MoH** after 8 h at 90 °C in benzene-d_6.

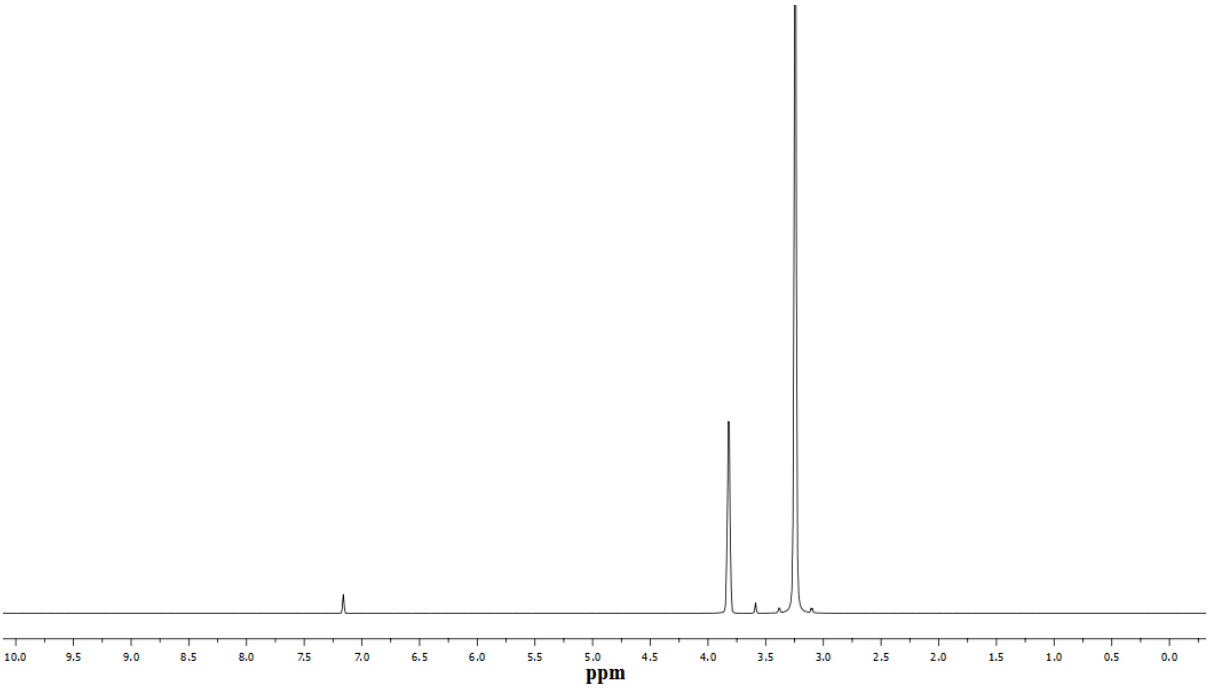

Figure S31. ^{1}H NMR spectrum of distilled methanol from the hydrolysis of CO_2 hydroboration products using 0.1 mol% **(κ^{6}-*P,N,N,N,C,P*-^{Ph_2PPr}PDI)MoH** in benzene-d_6.

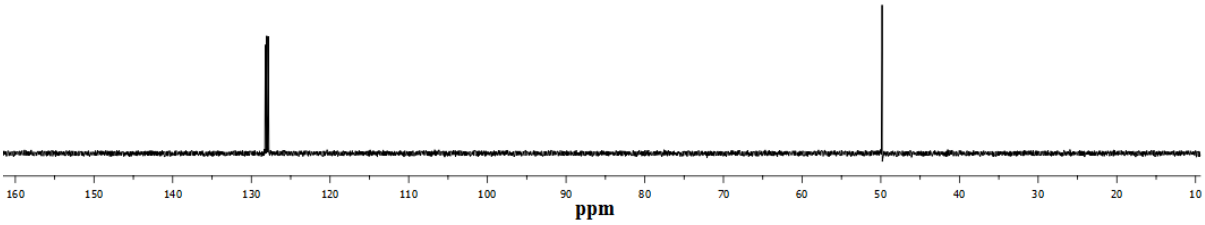

Figure S32. ^{13}C NMR spectrum of distilled methanol from the hydrolysis of CO_2 hydroboration products using 0.1 mol% **(κ^6-*P,N,N,N,C,P*-^{Ph_2PPr}PDI)MoH** in benzene-d_6.

UV-Vis Absorption Spectra:

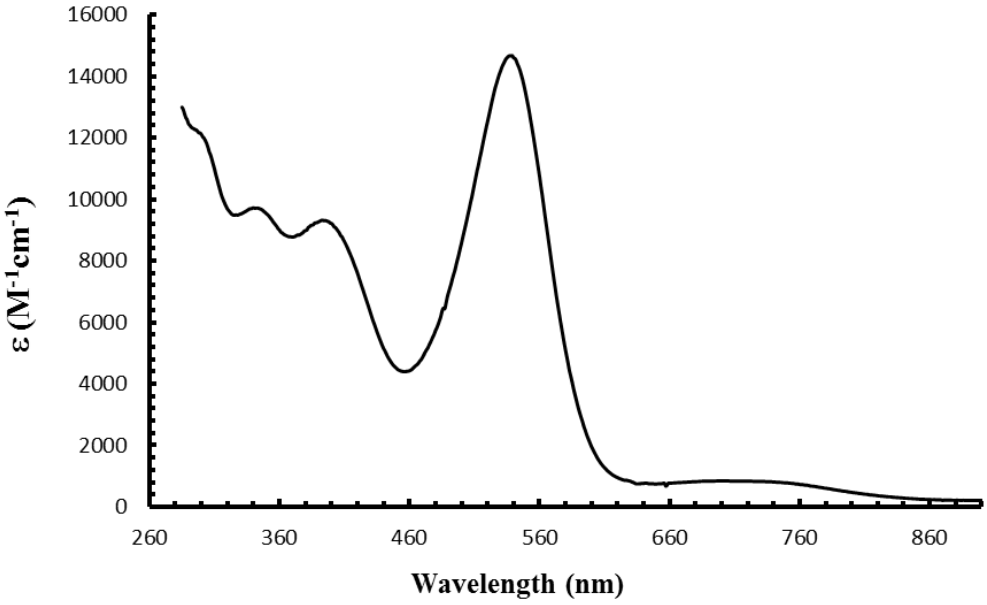

Figure S33. Absorption spectrum of **(^{Ph_2PPr}PDI)Mo(CO)** in THF. Molar absorptivity values have been determined from 5 independent concentrations.

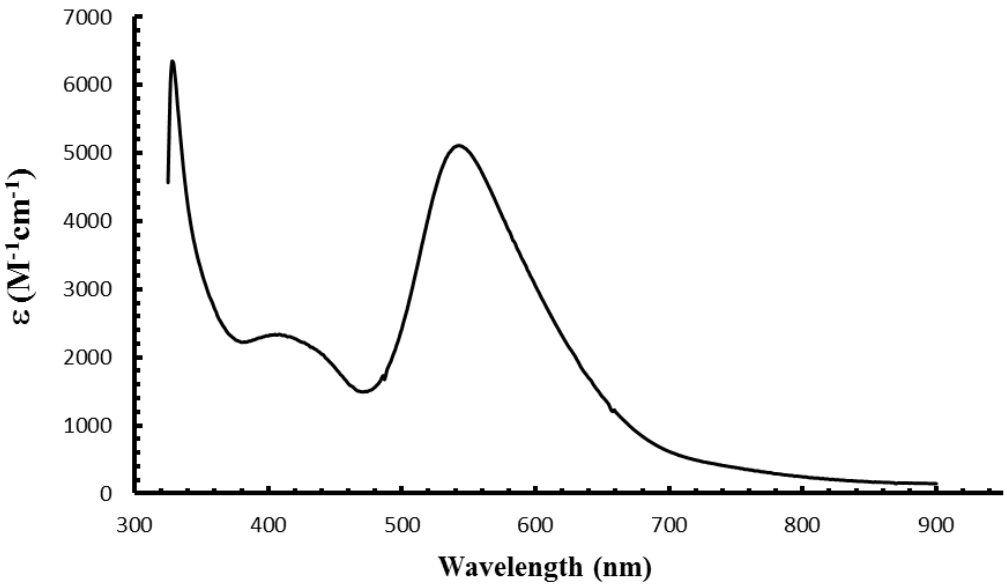

Figure S34. Absorption spectrum of **[(^{Ph_2PPr}PDI)MoI(CO)][I]** in acetone. Molar absorptivity values have been determined from 5 independent concentrations.

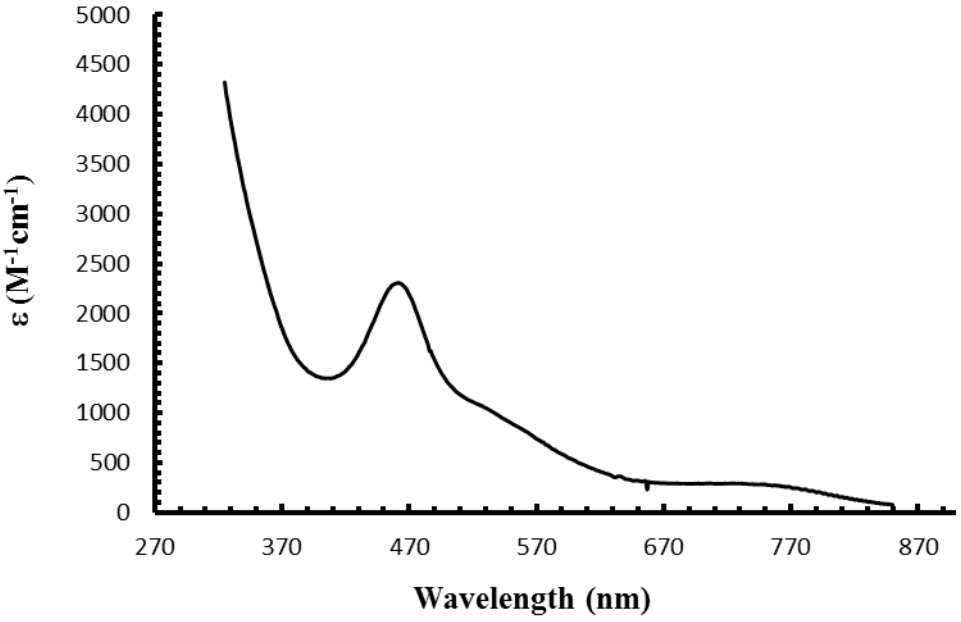

Figure S35. Absorption spectrum of **[(^{Ph_2PPr}PDI)MoI][I]** in acetonitrile. Molar absorptivity values have been determined from 5 independent concentrations.

Table S4. Wavelengths of maximum absorption (λ_{max}) and extinction coefficients (ε) for each complex analyzed by UV-vis spectroscopy.

Complex	λ_{max} (nm)	ε (M^{-1} cm^{-1})
(^{Ph_2PPr}PDI)Mo(CO)	299	12310
	345	9600
	399	9230
	537	14390
	723	830
[(^{Ph_2PPr}PDI)MoI(CO)][I]	328	6530
	410	2330
	541	5040
[(^{Ph_2PPr}PDI)MoI][I]	452	2300
	527	1030
	735	290